Genetic Reinstatement of RIG-I in Chickens Reveals Insights into Avian Immune Evolution and Influenza Interaction

Hicham Sid[1*], Theresa von Heyl[1], Sabrina Schleibinger[1], Romina Klinger[1], Leah Heymelot Nabel[1], Hanna Vikkula[1], Rodrigo Guabiraba[2], Vanaique Guillory[2], Ryan Scicluna[1], Mohanned Naif Alhussien[1], Brigitte Böhm[3], Benjamin Schade[3], Daniel Elleder[4], Samantha Sives[5], Lonneke Vervelde[5], Sascha Trapp[2], Benjamin Schusser[1,6]

[1] TUM School of Life Sciences, Weihenstephan, Department of Molecular Life Sciences, Reproductive Biotechnology, Technical University of Munich, 85354, Freising, Germany
[2] UMR ISP, INRAE, Université de Tours. 37380, Nouzilly, France
[3] Bavarian Animal Health Service, Department of Pathology, 85586, Poing, Germany
[4] Institute of Molecular Genetics of the Czech Academy of Sciences, Prague, Czech Republic
[5] Division of Immunology, The Roslin Institute and Royal (Dick), School of Veterinary Studies, University of Edinburgh, UK
[6] Center for Infection Prevention (ZIP), Technical University of Munich, 85354 Freising, Germany

*To whom correspondence may be addressed: Hicham Sid

Email: hicham.sid@tum.de

Author Contributions: H.S., T.v.H., S.Schleibinger, R.K., L.H.N., H.V., R.G., V.G., R.S., M.N.A., B.B., B. Schade, D.E., S. Sives, L.V., S.T., and B. Schusser contributed to the production of experimental data. H.S., T.v.H., S. Schleibinger, L.H.N., R.G., B.B., B. Schade, D.E., S. Sives, L.V., S.T., and B. Schusser contributed to experimental design and interpretation of the data. H.S., S.T., and B. Schusser wrote the manuscript.

Competing Interest Statement: The authors declare no competing interests.

Keywords: avian influenza virus, *RIG-I*, *RNF135*, transgenic chicken, duck.

This PDF file includes:

Main Text
Figures 1 to 9

Abstract

Retinoic acid-inducible gene I (*RIG-I*) activates mitochondrial antiviral signaling proteins, initiating the antiviral response. *RIG-I* and *RNF135*, a ubiquitin ligase regulator, are missing in domestic chickens but conserved in mallard ducks. The chickens' *RIG-I* loss was long believed to be linked to increased avian influenza susceptibility. We reinstated both genes in chickens and examined their susceptibility to infection with an H7N1 avian influenza virus. Uninfected *RIG-I*-expressing chickens exhibited shifts in T and B cells. At the same time, the H7N1 infection led to severe disease, persistent weight loss, and increased viral replication compared to wild-type chickens. The simultaneous expression of *RIG-I* and *RNF135* potentiated the *RIG*-I activity and was associated with exacerbated inflammatory response and increased mortality without influencing virus replication. Additional animal infection experiments with two other avian influenza viruses validated these findings. They confirmed that the harmful effects triggered by *RIG-I* or *RIG-I-RNF135*-expression require a minimum degree of viral virulence. Our data indicate that the loss of *RIG-I* in chickens has likely evolved to counteract deleterious inflammation caused by viral infection and highlight an outcome of restoring evolutionary lost genes in birds.

Significance Statement: The evolutionary loss of a crucial innate immune sensor like *RIG-I* in domestic chickens and its presence in closely related avian species such as ducks has long puzzled researchers. We genetically reinstated *RIG-I* in chickens, alongside its ubiquitination factor, *RNF135*, to uncover their roles in responding to influenza virus interactions in chickens. Our findings suggest that the loss of *RIG-I* in chickens may have occurred as an adaptive strategy to mitigate harmful inflammation associated with influenza infection. We shed light on an outcome of reinstating evolutionarily lost genes in birds and open new avenues for understanding immune responses in vertebrates.

Introduction

Avian influenza virus (AIV) is an epizootic pathogen with zoonotic potential (1) that recently caused devastating outbreaks worldwide, leading to the loss of millions of birds due to animal death and culling (2). The ability of the virus to spread between mammals and humans is highly concerning due to the potential risk of pandemics (3, 4). The viral

68 reservoir of AIVs are wild birds of the orders *Anseriformes* (ducks, geese, and swans) and
69 *Charadriiformes* (gulls and terns) (5), which, compared to chickens or other galliform birds,
70 exhibit milder clinical symptoms despite efficient viral replication (6). Certain genomic
71 features of the duck, including a functional retinoic acid-inducible gene I *(RIG-I)* gene,
72 were reported to be associated with their relative resistance to clinical avian influenza
73 infection (7). *RIG-I* is a cytosolic RNA sensor that recognizes and binds to the 5'
74 triphosphate end (5'-ppp) (8). It forms a first line of antiviral defense as a pathogen
75 recognition receptor (PRR) against RNA viruses (9). Upon activation, the *RIG-I* interacts
76 with the mitochondrial antiviral signaling proteins (MAVS), inducing a pro-inflammatory
77 antiviral response characterized by the upregulation of type I and type III interferons (IFNs)
78 followed by the expression of IFN stimulated genes (ISGs) (10). The activity of *RIG-I* is
79 believed to be controlled by post-translational modification of tripartite motif-containing
80 protein 25 (*TRIM25*) (11) and RING finger protein 135 (*RNF135*, also known as *Riplet* or
81 *REUL*). The latter was found to modify *RIG-I* by lysine 63-linked polyubiquitination of the
82 C-terminal region of the caspase activation and recruitment domain (CARD) (12), leading
83 to a stronger *RIG-I* signal transduction (13). The physiological role of mammalian *RIG-I*,
84 its function in viral infections, and its parallel evolution with other RLRs are well
85 documented (11, 14-16). Furthermore, the knockout (KO) of *RIG-I* in mice has shown that
86 this gene may have additional functions related to adaptive immunity (14). *RIG-I* KO mice
87 exhibited a defect in migratory dendritic cells in combination with a reduced frequency of
88 polyfunctional effector T cells upon influenza infection (17).

89 In ducks, *RIG-I* elicits a potent interferon (IFN) response within the first few hours after
90 infection, leading to survival against most AIV strains (18). In contrast, chickens lack *RIG-*
91 *I*, which probably lost its function in a common ancestor of galliform birds (7, 19).
92 Interestingly, a recent study detected disrupted *RIG-I* pseudogenes in some Galliformes,
93 including the helmeted guineafowl (*N. meleagris*) and the northern bobwhite (*C.*
94 *virginianus*) (20). Authors hypothesized a compensatory evolution of melanoma
95 differentiation-associated gene-5 (*MDA5*) that accompanied the gradual loss of *RIG-I* in
96 chickens (20). The evolutionary loss of *RIG-I* in different galliform birds correlated with the
97 simultaneous loss of its ubiquitin ligase *RNF135* (20), which has been described to be
98 critical for *RIG-I* ubiquitination in mammals, unlike *TRIM25*, which is increasingly believed
99 to be less important for *RIG-I* signaling (21). Reasons behind the loss of *RIG-I* and its

100 ubiquitination factor in chickens are still unknown and remain enigmatic, especially given
101 the virus-limiting effect of duck *RIG-I* overexpression in AIV-infected chicken DF-1 cells
102 (7).

103 To date, the effect of *in vivo* expression of *RIG-I* in chickens has never been studied, and
104 no transgenic chicken lines expressing duck *RIG-I* have been generated, likely due to the
105 lack of suitable biotechnological tools in avian research. Here, we used chicken primordial
106 germ cells (PGCs) to develop genetically modified chickens expressing duck *RIG-I* and
107 *RNF135* under the control of their respective duck promoters. The generated birds were
108 healthy and developed normally compared to their WT siblings. In the absence of infection,
109 we observed differences in adaptive immune cells of *RIG-I*-expressing chickens,
110 particularly T cell populations. In contrast, the co-expression of *RNF135* with *RIG-I*
111 contributed to a balanced adaptive immune phenotype that appeared to be similar to WT
112 birds. Infection experiments with an H7N1 AIV led to severe clinical disease associated
113 with a strong inflammatory response, high *IFN-γ* expression, and elevated viral replication
114 in *RIG-I*-expressing chickens compared to other challenged groups. In contrast, infected
115 *RIG-I-RNF135*-expressing chickens presented with inflammation and a differential
116 expression of *IFN* and pro-inflammatory cytokines compared to *RIG-I*-expressing
117 chickens. The obtained data reveal the immunological functions of *RIG-I* in chickens and
118 the benefit of learning from less susceptible species to influenza infection to improve the
119 immune system's resilience towards infection.

120
121 **Results**
122
123 **Generation of PGCs that express duck *RIG-I* and *RNF135* under the respective duck**
124 **promoters**

125 The genetic modification of PGCs represents a crucial step for generating transgenic
126 chickens. PGCs are the precursors of sperm and eggs in adult animals, and therefore, we
127 used them to produce chimeric roosters paired with WT layer hens to obtain the desirable
128 transgene. To generate chickens that express *RIG-I* and *RNF135*, we started by cloning
129 duck *RIG-I* and *RNF135*, which were subsequently inserted into two different expression
130 vectors. *RIG-I* and *RNF135* were expressed under their respective duck promoters and
131 used to generate PGCs expressing both genes separately. While the duck *RIG-I* promoter

132 was previously described (22), we determined the activity of the duck *RNF135* promoter,
133 which was examined by the generation of different deletion mutants tested in the
134 NanoDLR™ Assay System. Therefore, different deletion mutants were generated,
135 including p1577, p1001, p349, and p197. Since we did not detect a core promoter activity
136 of the duck *RNF135*, we used the full-length sequence of the duck *RNF135* for the
137 generation of duck *RNF135*-expressing PGCs (Fig. 1a). The assembled expression
138 vectors that were used to generate PGCs are presented in Fig. 1b.

139 Due to the unavailability of commercial antibodies for detecting the duck *RIG-I*, we inserted
140 a FLAG-Tag on the C-terminus to facilitate its detection using anti-FLAG antibodies. The
141 activity of the duck *RIG-I* was examined by differentiating the *RIG-I*-expressing PGCs into
142 PGC-derived fibroblasts (Fig. 1c, Supplementary Figure 1) that were infected with a low
143 pathogenic avian influenza virus (LPAIV) H9N2 (Fig. 1c). Results showed that the infection
144 led to activation of *RIG-I* as shown by FLAG-Tag staining. At the same time, the MOCK-
145 infected cells remained negative for *RIG-I* expression (Fig. 1c).

146 **The expression of *RIG-I* did not limit the viral replication under *in vitro* and *in ovo***
147 **conditions**

148 According to previously published data by Barber et al. (7), the overexpression of duck
149 *RIG-I* in chicken DF-1 cells reduced the replication of H5N2 or H5N1 viruses when cells
150 were infected at an MOI 1. Authors constitutively expressed *RIG-I* under the control of the
151 CMV promoter using expression vector pcDNA 3.1. Therefore, we wanted to examine if
152 the expression of *RIG-I* under the control of the duck RIG-I promoter can lead to a similar
153 effect in limiting virus replication. To this end, we isolated chicken embryonic fibroblasts
154 (CEFs) and produced embryonated eggs from the generated transgenic chickens and
155 infected them with LPAIV H9N2. After virus infection, supernatants and allantoic fluid were
156 collected from CEFs and embryonated eggs, respectively. We quantified the newly
157 produced viral particles using a focus-forming assay. Surprisingly, transgene expression
158 did not significantly affect the viral replication in both tested systems: CEFs (Fig. 1d,
159 Supplementary Figure 2) and embryonated chicken eggs (Fig.1e, Supplementary Figure
160 3), which was the opposite in the previously published study (7). This highlights the
161 importance of the chosen promoter, which may have affected the expression of *RIG-I* and
162 influenced the innate immune response towards influenza virus.

163 **Phenotypic characterization of the genetically modified chickens**

164 Upon the generation of *RIG-I-* and *RNF135*-expressing chicken lines, we wanted to ensure
165 that the genetic modification did not negatively affect the growth of the generated
166 transgenic birds. Therefore, we monitored their development by weekly measuring their
167 body weights (Fig. 2a). Both generated chicken lines showed comparable growth to their
168 WT siblings. The animals matured sexually, and no harmful phenotype was detected (Fig.
169 2a and 2b). The expression of both genes was examined via RT-PCR, revealing that both
170 genes are expressed differentially in various tissues (Fig. 2c). We also detected
171 comparable levels in expression levels with the duck (Fig. 2d)

172 Previous studies show that mammalian *RIG-I* affects adaptive immunity, mainly T cells
173 (17). Therefore, we sought to examine whether the re-expression of *RIG-I* in chickens will
174 have similar effects. We analyzed the number of peripheral blood mononuclear cells
175 (PBMCs) using flow cytometry to investigate the possible impact of expressing *RIG-I*,
176 *RNF135,* or both on immune cell counts. No differences were observed in the number of
177 immune cells between *RNF135*-expressing chickens and their WT siblings
178 (Supplementary Figure 4). However, *RIG-I*-expressing chickens exhibited a significantly
179 higher number of αβ and γδ T cells as well as B cells in comparison to their WT siblings
180 ($p<0.05$) (Fig. 2e). This was not the case for monocyte counts, where no significant
181 differences were observed (Fig. 2e). In addition, no significant differences were observed
182 in *RIG-I*-expressing chickens compared to WT birds regarding the levels of IgM and IgY
183 at 12 and 14 weeks of age (Supplementary Figure 5).

184 Further analysis of different T cell subpopulations indicated that *RIG-I*-expressing
185 chickens had a significantly higher number of CD4+T cells, CD8α^{neg}T cells and a
186 significantly lower number of CD8α+^{high}T cells ($p<0.05$) (Fig. 3a and 3b). T-cell activation
187 was quantified after lectin activation using Concanavalin A (ConA). *RIG-I*-expressing
188 chickens had a higher level of T cell activation in TCR1+/CD25+ T cells, which was not
189 the case for TCR2,3+/CD25+ T cells (Fig. 3c).

190 Heterozygous birds expressing each gene separately were crossed to obtain birds that
191 simultaneously express both genes *RIG-I* and *RNF135*. The obtained *RIG-I-RNF135*-
192 expressing chickens were monitored weekly for weight gain and closely investigated at
193 eight and twelve weeks of age for possible alternate immune phenotypes similar to those

194 observed in *RIG-I*-expressing birds. Unlike *RIG-I*-expressing chickens, no significant
195 differences in T cells or B cell counts were detected in *RIG-I-RNF135*-expressing chickens
196 in comparison to their WT siblings (Fig. 4d). Our analysis also comprised the investigated
197 cell populations in *RIG-I*-expressing birds including αβ, γδ and B cells (Fig. 4a).
198 Furthermore, we quantified CD4+, CD8+ T cells and corresponding subpopulations (Fig.
199 4b and Fig.4c). This was also the case for body weight gain, where no significant
200 differences were observed in *RIG-I-RNF135*-expressing chickens in comparison to WT
201 birds (Supplementary Figure 6).

202 These data indicate that the *RIG-I*, an innate immune sensor, can influence adaptive
203 immunity by causing shifts in T and B cell populations. In contrast, co-expression of
204 *RNF135* with *RIG-I* seems to balance the adaptive immune cell populations, comparable
205 to WT birds.

206 ***RNF135* is required for the potentiation of *RIG-I*'s activity**

207 The role of *RNF135* as an essential ubiquitination factor that supports the antiviral activity
208 of *RIG-I* was previously determined in mammalian cells (13). Later on, *RNF135* was found
209 to be the obligatory ubiquitin for *RIG-I* (23), while so far, this was not known in birds. We
210 investigated the effect of expressing *RNF135* on the antiviral activity of *RIG-I* in genetically
211 modified chickens. We examined the susceptibility of the generated transgenic lines
212 towards an H7N1 AIV, a direct precursor of a highly pathogenic avian influenza virus
213 (HPAIV), known to cause severe acute respiratory disease in chickens (24). Birds were
214 challenged with the virus and monitored for clinical signs, weight gain, viral replication,
215 and lesion development. *RIG-I*-expressing chickens had the highest rate of morbidity, as
216 indicated in Fig. 5a. The clinical symptoms started within the first two days of infection,
217 where the morbidity rate reached a significant rate of 44% at one-day post-infection (dpi)
218 ($p<0.05$) and increased to 67% at two dpi ($p<0.05$), which then decreased to 18% by three
219 dpi ($p<0.05$). The onset of clinical disease was accompanied by a significant weight loss
220 at two dpi that remained significantly low at six dpi ($p<0.05$) (Fig. 5c) and coincided with a
221 pulmonary lesion score that increased from 0.8 at two dpi to 2.3 at six dpi (Fig. 6a and 6b).
222 This was also confirmed by histological assessment of the caecum that revealed necrotic
223 lesions associated with pronounced epithelial hyperplasia (Fig. 6b). *RIG-I-RNF135*-
224 expressing chickens exhibited increasing clinical illness, from 13% of sick animals at one

225 dpi to 50% at three dpi ($p<0.05$). Severe and prolonged clinical symptoms associated with
226 mortality in this group lasted until six dpi.

227 The expression of *RNF135* alone resulted in a mortality rate comparable to WT birds. In
228 contrast, the clinical symptoms in *RNF135*-expressing chickens lasted till three dpi with a
229 total of 25% sick animals (Fig. 5b). This was not the case for WT chickens that exhibited
230 clinical symptoms only for the first two days after infection and had a morbidity rate of 13%
231 and 19% at one and two dpi, respectively (Fig. 5b).

232 The quantification of the virus genome copies via qRT-PCR showed that the expression
233 of *RIG-I* together with *RNF135* significantly reduced the amount of viral genome copies in
234 the caecum compared to *RIG-I* expressing chickens at two and six dpi ($p<0.05$) (Fig. 5d).
235 In the lung, challenged *RIG-I-RNF135*-expressing chickens displayed a virus replication
236 rate similar to WT birds and a significantly lower replication rate than *RIG-I*-expressing
237 chickens at two dpi ($p<0.05$). Conversely, *RIG-I*-expressing chickens had the highest viral
238 replication rate in the lung and the caecum among all investigated groups, with a
239 significant difference compared to *RIG-I-RNF135*-expressing chickens ($p<0.05$) (Fig. 5d).
240 The amount of viral nucleic acid remained at a high level at six dpi, indicating the lack of
241 viral clearance in these birds, which was not the case for the other challenged chicken
242 lines (Fig. 5d).

243 These results indicated that the reinstatement of *RIG-I* or *RIG-I-RNF135*-expressing
244 chickens had no effect on viral replication compared to WT birds. The different outcome
245 in viral replication in *RIG-I-RNF135*-expressing chickens, compared to *RIG-I*-expressing
246 chickens, confirms the role of *RNF135* as a ubiquitin ligase at the early stage of infection.
247 Also, it demonstrates that the chicken *TRIM25* does not overtake the role of *RNF135* in
248 *RIG-I*-expressing chickens.

249 **The expression of *RIG-I* and *RNF135* in H7N1-challenged birds coincided with the**
250 **acute phase of infection**

251 We aimed to quantify possible changes in the expression levels of both transgenes in the
252 challenged animals after the H7N1 infection. We quantified *RIG-I* and *RNF135*
253 expressions via qRT-PCR in the lung and the caecum (Fig. 5e). The caecal expression of
254 *RIG-I* in virus-infected *RIG-I-RNF135* chickens was increased by ~26 fold. At the same

255 time, infected *RIG-I* chickens exhibited an increase of ~24-fold compared to *RIG-I-*
256 *RNF135* MOCK controls. Infected *RIG-* and *RIG-RNF135*-expressing chickens had a
257 comparable *RIG-I* expression to *RIG-RNF135*-MOCK controls with no significant
258 upregulation (Fig. 5e). Overall, we observed lower expression of *RNF135* in the caecum
259 and lungs compared to *RIG-I-RNF135*-MOCK controls. The expression increased by 1.4
260 fold in *RNF135*-infected birds and ~2 fold in *RIG-I-RNF135*-infected chickens. In the lung,
261 the *RNF135* expression at two dpi was upregulated by ~6 fold and ~4 fold in infected
262 *RNF135* and *RIG-I-RNF135*-expressing chickens, respectively. At six dpi, the *RNF135*
263 expression was at a comparable level with the *RIG-I-RNF135* MOCK controls (Fig. 5e).
264 These data indicate that the infection led to a quick upregulation of *RIG-I* at the acute
265 phase of infection, which quickly decreased afterward.

266 **Differential regulation of innate immune genes in naïve as well as in H7N1-**
267 **challenged *RIG-I*, *RNF135,* and *RIG-I-RNF135*-expressing chickens**

268 We speculated that the observed acute inflammatory reaction could be due to a differential
269 regulation of inflammatory genes related to *RIG-I* signaling. Therefore, we sought to
270 quantify the differentially expressed genes (DEGs) between transgenic and WT birds. We
271 used the Fluidigm qRT-PCR array to identify changes in the expression of selected innate
272 immune genes in both naïve and H7N1-challenged birds (25). The results revealed that in
273 the absence of infection, *RIG-I-RNF135*-expressing chickens already had a significantly
274 higher expression of ISGs in the caecum, including *ISG12-2* and *OASL,* as well as the
275 transcription factor Early Growth Response *1 (EGR1)* (Fig. 7a, Supplementary Figure 7).
276 In contrast, others, including *EGR1*, interleukin 4 induced 1 (*IL4I1)*, Interleukin-1 beta
277 (*Il1β),* and Interleukin 8 (*IL8),* were significantly upregulated in the spleen (Fig. 7a and
278 Supplementary Figure 7).

279 The comparison of challenged groups with non-infected controls (WT-MOCK) indicated
280 that *RIG-I* chickens expressed several inflammatory genes in the caecum and lungs that
281 were not expressed in the other groups. This included *IFITM1*, *IL6,* and *LIPI* (Fig. 7b,
282 Supplementary Figure 7c and 7d). At two dpi, we observed the upregulation of genes
283 involved in the JAK-STAT signaling pathway, including *IL-6* and *STAT3,* which was not
284 the case at 6 dpi (Fig. 7b, 7c, and 7d). The significant upregulation of inflammatory and
285 immune regulatory genes in the *RIG-I*-expressing chickens persisted until six dpi, where

286 over 20 genes were exclusively upregulated in the spleen (Fig. 7e and Supplementary
287 Figure 7e). This was not the case for *RIG-I-RNF135*-expressing chickens and WT
288 chickens with an exclusive expression of three and seven genes, respectively (Fig. 7e and
289 Supplementary Figure 7e). In addition, the analysis of expressed genes in the spleen
290 revealed that only *RIG-I-RNF135* chickens expressed *IRF7* and *TRIM25*, in contrast to
291 *RIG-I*-expressing chickens (Fig. 7e and Supplementary Figure 7e).

292 The functional enrichment analysis of the genes involved in the biological processes of
293 transgenic chickens indicated that the regulated genes in *RIG-I*-expressing chickens were
294 highly involved in metabolic activities. In contrast, those in *RIG-I-RNF135*-expressing birds
295 were primarily involved in regulatory mechanisms (Supplementary Figure 8). Overall, the
296 obtained data confirm that *RIG-I*-expressing chickens exhibited a significant increase of
297 inflammatory cytokines that were not observed in other challenged birds, which may
298 explain the acute inflammatory reaction in these birds.

299 **High expression of *IFN-γ* is associated with significant virus replication in *RIG-I-***
300 **expressing birds**

301 Since we observed a significant reduction of viral genome copies in the *RIG-I-RNF135*-
302 expressing chickens compared to *RIG-I*-expressing birds, we compared the DEGs
303 between H7N1-infected groups. This helped us determine possible factors behind the
304 increased H7N1 replication in *RIG-I*-expressing birds. Interestingly, these birds lacked
305 interferon upregulation compared to infected WT birds or *RIG-I-RNF135*-expressing
306 chickens (Fig. 8a). We also found that the viral infection led to a significant increase in the
307 expression of *IFN-γ* at six dpi when compared to H7N1-infected *RIG-I-RNF135*-expressing
308 chickens (14-fold change increase) and WT birds (9-fold change increase) (Fig. 8b and
309 8d) ($p<0.05$). In contrast, *RIG-I-RNF135*-expressing birds quickly exhibited a significant
310 increase of *IFN-α* expression, already at two dpi, in comparison to *RIG-I*-expressing birds
311 (12-fold change) as well as to WT birds (17-fold change) (Fig. 8c). We concluded that the
312 co-expression of *RNF135* and *RIG-I* in chickens leads to a significant increase of *IFN-α*
313 expression, which was not observed when *RIG-I* was expressed solely. In addition, *RIG-*
314 *I*-expression caused an upregulation of *IFN-γ* (Fig. 8b and 8d) that was accompanied by
315 a significant increase in virus genome copies.

316

317 **The deleterious inflammatory response in *RIG-I* and *RIG-I-RNF135*-expressing**
318 **chickens depends on the virulence of the influenza subtype**

319 The infection with H7N1 revealed a unique phenotype that manifested in acute
320 inflammation and increased mortality in *RIG-I* and *RIG-I-RNF135*-expressing chickens.
321 Hence, we were interested in investigating the effect of reinstating *RIG-I* and *RNF135* in
322 the chicken genome on the outcome of infection with two additional virus strains of high
323 or low virulence. We conducted two additional *in vivo* infection studies using two viruses:
324 an H3N1 (A/chicken/Belgium/460/201) and an H9N2 (A/chicken/Saudi Arabia/CP7/1998).
325 While both subtypes are classified as low pathogenic AIVs due to their monobasic
326 hemagglutinin cleavage sites, H3N1 has been described as a highly virulent strain causing
327 severe clinical infection and mortality in adult layers (26). Displaying a distinct tropism for
328 the hen's oviduct, H3N1 causes salpingitis and peritonitis, which are associated with a
329 severe drop in egg production. In contrast, the H9N2 virus is effectively low virulent and
330 does not cause any detectable symptoms in experimentally infected chickens(27). The
331 H9N2- and H3N1- infection experiments of *RIG-I* and *RIG-I-RNF135*-expressing chickens
332 revealed major differences in the outcome of infection between the two viruses. While
333 H9N2 infection did not cause any clinical disease in the *RIG-I* or *RIG-I-RNF135*-
334 expressing chickens (Supplementary Figure 9), infection with H3N1 led to marked
335 clinical/pathological disease signs and disease aggravation, similar to those observed in
336 the H7N1 infection experiment. The infection with H3N1 led to early clinical disease and
337 mortality onset that were more pronounced in *RIG-I*-expressing birds (Fig 9a, 9b and
338 Supplementary Figure 10). However, we did not detect differences in viral RNA loads in
339 tracheal swabs between the H3N1-infected groups except for 7dpi, where *RIG-I*-
340 expressing birds exhibited significantly higher loads compared to WT birds (Fig. 9a). *RIG-*
341 *I*-expressing chickens also manifested a significantly increased expression of *IL-1*β, *IL6*,
342 *IFN-*α and *IFN-*γ compared to the other infected birds (Fig. 9c). The assessment of
343 histological lesions of the reproductive system indicated that the infection with H3N1 led
344 to pronounced atrophy in *RIG-I* and *RIG-I-RNF135*-expressing birds in comparison to WT
345 birds (Fig. 9d), accompanied by fibrinous peritonitis, salpingitis and vasculitis (Fig. 9e).
346 These data confirm the observations made with H7N1 regarding the harmful inflammation.
347 They indicate that the deleterious clinical disease caused by *RIG-I* reinstatement depends
348 on the degree of viral virulence.

349 **Discussion**
350
351 The constant arms race between pathogens and the host affects different aspects of the
352 immune system, including innate sensors. The reason for the loss of *RIG-I* in Galliformes,
353 which correlated with the disappearance of the ubiquitin ligase *RNF135*, remained a
354 mystery (20), especially given the established contributing role of *RIG-I* in the resilience
355 towards influenza in ducks and other species (7, 28). It was previously speculated that the
356 gradual loss of *RIG-I* and *RNF135* in the chicken was possibly caused by the pathogen's
357 resistance to the innate sensor or the disappearance of some relevant pathogens (20). At
358 the same time, preservation of the antiviral competence accompanied the loss of *RIG-I*
359 and *RNF135* in chickens via the evolutionary selection of *MDA5* and *LGP2* (29). The
360 beneficial effect of the duck *RIG-I*-overexpression in chicken DF-1 cells was demonstrated
361 by the limited replication of AIV in these transgene-expressing cells (7). So far, no chickens
362 expressing the duck *RIG-I* have been generated to investigate their antiviral response *in*
363 *vivo*. In this study, we produced genetically modified chickens that express *RIG-I* with or
364 without its ubiquitin ligase *RNF135* to examine the physiological role of both genes and
365 their function during AIV infection. Both genes were cloned from the duck representing the
366 most studied avian influenza reservoir with evolutionary conserved *RIG-I* and *RNF135* (6,
367 20, 30). The expression of both genes was controlled under their respective duck
368 promoters since the duck *RIG-I* was previously tested in chicken cells(22). This strategy
369 allows the strict control of gene expression that can be induced only upon infection, which
370 prevents undesirable production of inflammatory cytokines that may cause autoimmune
371 diseases (22). While the duck *RIG-I* promoter was previously identified (22), we described
372 the activity of the duck *RNF135* promoter using chicken cells.

373 Without infection, *RIG-I* expression did not cause any harmful phenotype, but led to
374 different adaptive immune cell counts compared to WT siblings. This suggests the role of
375 the *RIG-I* in priming T cell immunity in the chicken, which can be similar to mice that
376 exhibited a lack of T cell immunity associated with deficiencies in migratory dendritic cell
377 activation, viral antigen presentation and CD8+ and CD4+ T cell priming (17) (14). In the
378 case of *RIG-I-RNF135*-co-expression, the balanced adaptive immune phenotype implies
379 a possible role of *RNF135* in modulating the T cell immune response in birds, which was
380 previously described for Th1 response and cytotoxic T cells in mice (31). Moreover, naïve
381 *RIG-I-RNF135*-expressing chickens had a significantly higher expression of interleukin 4

382 inducible gene 1 (*IL4I1*) as well as protein nuclear translocation 7 *(IRF7*) and tripartite
383 motif-containing protein 29 *(TRIM29)*. This may explain the differential adaptive immune
384 phenotype between *RIG-I* and *RIG-I-RNF135*-expressing chickens. Previous studies
385 indicated the involvement of *IL4I1* in the signaling to T and B lymphocytes (32) and the
386 effective role of translocation factors such as *IRF7* in chicken cells transfected with the
387 duck *RIG-I* (22).

388 The lack of an antiviral effect after *in ovo* and *in vitro* experimental infections with LPAIV
389 H9N2 was discordant with the previously described antiviral effect of duck *RIG-I* in chicken
390 DF-1 cells (7). Barber et al, observed low virus replication upon the overexpression of
391 *RIG-I* under the control of the CMV promoter. The difference between our results and
392 previously published data can be related to the chosen promoter used by Barber et al,
393 which may lead to a higher upregulation of *RIG-I* and, consequently, a strong production
394 of interferon-stimulated genes. Additional factors can stand behind the differences
395 between the previously published results by Barber et al(7), and our data, including
396 influenza subtypes and the type of cells.

397 H7N1-challenge experiments of the generated transgenic birds revealed that *RIG-I-*
398 expressing chickens had an early upregulation of proinflammatory cytokines such as *IL-*
399 *6*, known to support *IL1β* in suppressing regulatory T cells, which can lead to an
400 uncontrolled increase in the number of CD4+ T cells (33). Furthermore, the expression of
401 *RIG-I* without *RNF135* was not beneficial in limiting H7N1 replication since the *RIG-I-*
402 expressing chickens had the highest viral genome copies among all challenged groups.
403 The requirement of *RNF135* for an *RIG-I*-mediated antiviral effect in *RIG-I-RNF135-*
404 expressing chickens was also described in mammalian cells (13). In addition, we found
405 that the H7N1 infection caused a significant upregulation of *RIG-I* in the caecum compared
406 to the lungs. This can be because *RIG-I* expression rapidly occurs upon stimulation and
407 may reach a peak by three hours post-infection (34). Similar observations were described
408 by Cornelissen et al. that detected a significant upregulation of *RIG-I* expression in the
409 lungs of ducks at 8h post H7N1 infection that significantly decreased at two dpi (35). *RIG-*
410 *I*-expressing birds infected with H7N1 exhibited an acute inflammatory response and
411 weight loss at two dpi, lasting till six dpi. Pang et al, reported that influenza virus could
412 hijack the inflammatory reaction associated with RIG-I signaling for its replicative
413 advantage, particularly in the respiratory tract (15). H7N1-infected *RIG-I*-expressing birds

414 showed several regulated immune genes compared to other infected groups, including
415 upregulation of the suppressor of cytokine signaling 1 (*SOCS1*) in the caecum. This may
416 explain the significant increase in viral genome copies and the observed T cell phenotype
417 since *SOCS1* is a potent inhibitor of JAK/STAT signaling (36) and is involved in several
418 mechanisms that regulate the T cell maturation, differentiation, and function (37).
419 Furthermore, the assessment of the immunophenotype of *RNF135*-expressing chickens
420 revealed differential upregulation of various genes, which suggests that this gene, on its
421 own, may function independently from *RIG-I* (38).

422 Interestingly, we detected significant upregulation of *IFN-γ* in the lungs of infected *RIG-I-*
423 expressing chickens compared to infected *RIG-I-RNF135-* and WT-chickens, which can
424 be responsible for lung-mediated injury and acute death caused by respiratory distress.
425 Similarly, H3N1 infection caused a relative upregulation of *IFN-γ* in the spleen and the
426 duodenum of *RIG-I*-expressing chickens. The role of *IFN-γ* was previously described in
427 *IFN-γ* KO mice that were less susceptible to lung inflammation and pathology upon
428 influenza infection (39). The lack of an antiviral effect in *RIG-I*-expressing chickens may
429 also indicate that chicken *TRIM25* is dispensable for *RIG-I* efficient ubiquitination. Similar
430 findings were described using human lung adenocarcinoma epithelial cells, where *TRIM25*
431 did not participate in the endogenous *RIG-I*-dependent antiviral responses (21). However,
432 other studies done in mammalian models indicated that the deletion of *TRIM25* increases
433 the susceptibility to influenza infection (40), supporting the evidence that *TRIM25* may
434 bind directly to the viral RNA, thereby contributing to the restriction of influenza virus
435 infection (41). The exacerbated inflammatory reaction in *RIG-I*-expressing chickens could
436 be related to the absence of *RNF135*, which suggests a stabilizing role of *RNF135*
437 comparable to *TRIM25* (42), though this requires further investigation. The increased
438 mortality rates in *RIG-I-* and *RIG-I-RNF135*-expressing chickens may be explained by
439 immunopathology in both chicken lines, despite the differences in viral replication. The
440 additional *in vivo* experimental challenge with the highly virulent H3N1 virus confirmed the
441 deleterious immunophenotype observed for the H7N1 virus, as demonstrated by the
442 upregulation of various inflammatory genes, including *IFN-γ, IFN-α, IL1β, and IL6*. The
443 absence of a similar phenotype after infection with the mildly virulent H9N2 virus revealed
444 that disease exacerbation in *RIG-I-* and *RIG-I-RNF135*-expressing chickens requires a
445 certain degree of viral virulence.

446 Our data suggest that the evolutionary loss of *RIG-I* in chickens and other galliform birds
447 was advantageous in coping with viral infections caused by AIV or other avian RNA
448 viruses. This subsequently helped decrease the acute inflammation and the damage to
449 the host. A comparable hypothesis was made in the case of pangolins that lost the *MDA5*
450 as an evolutionary mechanism to cope with coronavirus-induced inflammation (43). The
451 acute inflammation seen in the generated chickens may be linked to the duplicated
452 function in RNA sensing due to the positive selection of *MDA5* (20), which could
453 exacerbate the inflammatory response and requires further investigation. Above that, we
454 propose that the antiviral role of *RIG-I* in ducks (7) is not exclusively related to this gene.
455 Still, it may involve the ubiquitination factor *RNF135* and possibly other unknown
456 regulatory factors that support *RIG-I* signaling and reduce the repercussions of acute
457 inflammation by negatively regulating *RIG-I* signaling (44). We provided novel information
458 regarding the outcome of the re-introduction of *RIG-I* and its ubiquitination factor *RNF135*
459 in the chicken genome. Future work should focus on identifying factors that can help
460 reduce the acute inflammatory reaction in *RIG-I-RNF135*-expressing chickens while
461 maintaining potent antiviral activity, which can lead to the generation of avian influenza
462 virus-resistant chickens.

463 **Materials and Methods**
464
465 **Cloning of the duck *RIG-I* and the duck *RIG-I* promoter**

466 Total RNA was isolated from the spleen of the mallard duck (*Anas platyrhynchos*) using
467 ReliaPrep™ RNA Tissue Miniprep System (Promega, USA), followed by cDNA synthesis
468 using GoScript™ Reverse Transcription System (Promega, USA) according to the
469 manufacturer's instructions. The duck *RIG-I* was amplified using Q5® High-Fidelity DNA
470 Polymerase (New England Biolabs, USA) using the primers 562_RIG-I_for (5'-
471 ATGACGGCGGACGAGAAGCGGAGC-3') and 563_RIG-I_rev (5'-
472 CTAAAATGGTGGGTACAAGTTGGAC-3') that were previously described (45). The PCR
473 thermal conditions were as follows: 98 °C 30 sec, followed by 35 cycles of 98 °C 10 sec,
474 67 °C 20 sec, 72 °C 1:30 min, and a final extension step of 72 °C 2 min.

475 The entire length of the duck *RIG-I* promoter was amplified using primers 706_RIG-I_For
476 (5'-AGCTGATGACCTGCAAAAAGTT-3') and 661_RIG-I_Rev (5'-
477 GGCTGGGCTCTGCCGGCCG-3'), which were described elsewhere (22). This resulted

478 in an amplicon of 2017 bp that was fully sequenced and aligned with the duck genome
479 (*Anas platyrhynchos*, NC_040075.1). The PCR was conducted following the following
480 thermal conditions 98 °C 30 sec, followed by 35 cycles of 98 °C 10 sec, 70 °C 20 sec,
481 72 °C 1:30 min, and a final extension step of 72 °C 2 min.

482 **Cloning of the duck *RNF135***

483 The genomic region containing duck *RNF135* was obtained from the GenBank contig
484 PEDO01000017.1 and corrected based on multiple publicly available duck RNAseq data.
485 Although the *RNF135* sequence was correctly predicted in many birds, we detected a
486 partially incomplete annotated sequence of the duck *RNF135*, specifically the missing 5'
487 part that contains the RING domain (previous accession number XM_013092775), while
488 the predicted version of the *RNF135* was made available (XM_027471415.2). The full-
489 length sequence of the duck *RNF135* was synthesized after codon optimization using the
490 IDT online tool (IDT™, USA) (Supplementary Figure 11). The obtained *RNF135* sequence
491 was subsequently cloned into the *RNF135*-expression vector driven by the duck *RNF135*
492 promoter (Fig. 1b).

493 **Identification of the duck *RNF135* promoter via Nano-Glo® Dual-Luciferase®**
494 **Reporter Assay**

495 The putative duck *RNF135* promoter was obtained by amplifying 1577 bp 5' of the ATG
496 start codon from duck gDNA cloned into pGEM vector (Promega, USA) and analyzed by
497 Sanger sequencing. The PCR was done using Q5® High-Fidelity DNA Polymerase with
498 primers: 707_RNF_Prom_For (5'-GA GCA GAG CCA GGC AGC TAT A-3'), 708 (5'-GGT
499 CCT GCT CGG GGC GGA GC-3') resulting in an amplicon of 1557 bp. The PCR thermal
500 conditions were conducted using Q5® High-Fidelity DNA Polymerase (New England
501 Biolabs, USA) at two step-PCR 98 °C 30 sec, 98 °C 10 sec, 72 °C 60 sec and a final
502 elongation step of 72 °C 2 min.

503 The promoter activity of duck *RNF135* was assessed by measuring promoter-driven
504 NanoLuc™ luciferase activity normalized to the luminescence of Firefly luciferase. To this
505 end, a total of 50.000 chicken DF-1 cells were seeded in 24 well plates and were co-
506 transfected 24h later with a vector plasmid containing the deletion mutant and a second
507 plasmid for the expression of Firefly under the PGK promoter (Promega, USA). 24h after

508 transfection, cells were washed with PBS, trypsinized, and resuspended in 250µl culture
509 medium. Firefly signal was detected by mixing 80µl of the cell suspension with the same
510 amount of ONE-Glo™ EX Reagent, prepared by combining ONE-Glo™ EX Luciferase
511 Assay Buffer with ONE-Glo™ EX Luciferase Assay Substrate in 1:1 ratio (Promega, USA).
512 After measuring the signal of the Firefly luciferase in the GloMax® 20/20 Luminometer
513 (Promega, USA), 80 µl NanoDLR™ Stop & Glo® reagent, prepared by adding
514 NanoDLR™ Stop & Glo® Substrate 1:100 into NanoDLR™ Stop & Glo® Buffer (Promega,
515 USA), were added to the samples. These were incubated for 10, 30, 60, and 120 min and
516 measured again in the GloMax® 20/20 Luminometer (Promega, USA) to detect the
517 NanoLuc™ Luciferase. The cell-free culture medium was used as a blank control.

518 **Determination of the Transgene Copy Number by Droplet Digital PCR**

519 Droplet digital PCR (ddPCR) was used to select PGC clones with a single genomic
520 transgene integration and was performed as described previously with slight modifications
521 (46). Briefly, 500ng of gDNA was digested with 20 units XbaI (New England Biolabs,
522 Germany) for one h, followed by an inactivation step at 65°C for 20 min. The Taqman PCR
523 reaction was set up using 10ng digested DNA, 2× ddPCR supermix for probes (no dUTP)
524 final concentration 1× (Bio-Rad Laboratories, USA), a 20× target primer/FAM-labeled
525 probe mix, and a 20× reference primer/HEX-labeled probe mix, which was followed by
526 droplet generation using the QX200 Droplet Generator by mixing 20ul of the TaqMan PCR
527 reaction with 70ul droplet generator oil in a DG8 Cartridge. The cycling conditions
528 comprised a 95°C for 10min, followed by 40 cycles of 94°C for 30 sec, 59°C for 60 sec,
529 and a final hold for 98°C for 10 min with a 2°C/s ramp rate at all steps. The copy number
530 was determined by calculating the proportion of positive and negative droplets using a
531 QX200 droplet reader, which was then analyzed using Quantasoft software (Bio-Rad
532 Laboratories, USA) (Supplementary Figure 1). The hygromycin fluorescent labeled-probe
533 ([5′FAM-TCGTGCACGCGGATTTCGGCTCCAA-3′] along with the primers: ddHygro_F
534 [5′-CATATGGCGCGATTGCTGATC-3′] and ddHygro_R [5′-
535 GTCAATGACCGCTGTTATGC-3′]). As a reference gene, we used the beta-actin probe
536 ([5′HEX-GTGGGTGGAGGAGGCTGAGC-BHQ3′] along with the primer combination
537 ddBeta_actin_F: [5′-CAGGATGCAGAAGGAGATCA-3′] and ddBeta_actin_R: [5′-TCC
538 ACCACTAAGACAAAGCA- 3′]). The quantification was done using the QX100 system
539 (Bio-Rad Laboratories, USA) (Supplementary Figure 1).

540

541 **Stimulation of duck *RIG-I* expression in PGC-derived fibroblasts**

542 The generated *RIG-I*-expressing PGCs were differentiated into fibroblasts (PGCFs) as
543 previously described (47) and subsequently infected with a LPAIV H9N2 to examine the
544 ability of *RIG-I* to detect its ligand. Briefly, 50.000 cells were seeded into 48 well plates
545 and infected with an MOI of 0.1 for 18h before they were fixed and stained using
546 immunofluorescence, as previously described (48). Cells were fixed with 4% PFA and kept
547 on ice for 10 min. Subsequently, they were washed with PBS and permeabilized with 0.5%
548 Triton X. The FLAG-Tag was detected by using a mouse anti-FLAG antibody
549 (Supplementary Table 1) that was incubated for 1h, followed by staining with goat anti-
550 mouse Alexa 568 (Supplementary Table 1). Slides were subsequently covered with a
551 mounting medium that contains DAPI for staining the nucleus and covered with coverslips
552 (Vector Laboratories, Inc., USA). Fluorescence microscopy was performed with a
553 fluorescence microscope (ApoTome, Zeiss).

554 **Generation of *RIG-I*-and *RNF135*-expressing chickens**

555 White Leghorn layer chickens (Lohmann selected White Leghorn (LSL), Lohmann-
556 Tierzucht GmbH, Cuxhaven, Germany) were used to generate transgenic chicken lines.
557 Animal experiments were approved by the government of Upper Bavaria, Germany (ROB-
558 55.2-2532.Vet_02-18-9). Experiments were performed according to the German Welfare
559 Act and the European Union Normative for Care and Use of Experimental Animals. All
560 animals received a commercial standard diet and water *ad libitum*. PGCs that express
561 either *RIG-I* or *RNF135* were generated using the DNA constructs shown in Fig. 1b, as
562 previously described (49, 50). To ensure the stable integration of the transgene, we used
563 the phiC31 integrase-mediated integration (51). Briefly, LSL PGCs were derived from the
564 blood of male embryonic vasculature at stages 13-15, according to Hamburger and
565 Hamilton (52). They were cultured at 37°C in a 5% CO2 environment using modified KO-
566 DMEM as described previously (53). A total of $5x10^6$ cells per transgene were washed
567 with phosphate-buffered saline (PBS) and resuspended in 100µl Nucleofector™ Solution
568 V (Lonza, Germany) containing the expression vector (Fig. 1b) and the integrase
569 expression construct. Electroporation was performed using an ECM 830 Square Wave
570 Electroporation System (BTX, USA), applying eight square wave pulses (350V, 100µsec).

571 After clonal selection using puromycin for *RIG-I* and blasticidin for *RNF135*, PGCs were
572 genotyped and tested for clones with one single genomic integration, which were then
573 used to generate the chimeric roosters. A total of 3000 cells with the desired genetic
574 modification were injected into the vasculature of 65h old embryos, transferred into a
575 surrogate eggshell, and incubated until the hatch. Upon sexual maturity, sperm was
576 collected from chimeric roosters for genotyping. (50, 54). The germline-positive roosters
577 were bred with wild-type hens to obtain heterozygous animals (the germline transmission
578 rate is presented in Supplementary Table 2).

579 The examination of the inheritance of duck *RIG-I* and the genotyping of the offspring was
580 done via PCR using FIREPol DNA Polymerase (Solis Biodyne) using the primer
581 combination 613_RIG-I-for (5'-CCTAGGAGAAGCATTCAAGGAG-3') and 563_RIG-
582 I_Rev (5'-CTAAAATGGTGGGTACAAGTTGGAC-3'). The following PCR conditions were
583 used: initial denaturation at 95 °C 3 min, followed by 40 cycles of 95 °C 30 sec, 60 °C 30
584 sec, 72 °C 20 sec, and a final extension step of 72 °C 5 min, resulting in a fragment of
585 298bp. The inheritance of the duck *RNF135* was examined using the primers combination
586 1121_RNF_For (5'GCATGGGATCAACCGACAGCATC-3') and 1017_RNF_rev
587 (5'CCACACACCAACTTGACTCGGTC-3', using the following PCR conditions 95 °C 3
588 min, followed by 40 cycles of 95 °C 30 sec, 60 °C 30 sec, 72 °C for 1 min and a final
589 extension step of 72 °C 5 min, resulting in an amplicon of 931bp.

590 Following the generation of different transgenic lines, they were monitored till sexual
591 maturity for possible harmful phenotypes that could been reflected in weight gain or the
592 ability to produce sperm or eggs. In addition, the immunophenotype of the generated birds
593 was assessed at 2, 5, 8, and 12 weeks after hatch by flow cytometry.

594 **Isolation, culture, and infection of chicken embryonic fibroblasts (CEFs)**

595 CEFs were isolated from 10-day-old (ED10) embryos according to the protocol published
596 elsewhere (55). Before the isolation of CEFs, embryos were genotyped by collecting blood
597 at ED10 and preparing a window of 0.5 cm^2 in the eggshell that allowed access to the
598 embryonic vasculature. CEFs were cultured using Iscove's liquid medium containing
599 stable glutamine (Biochrom, Germany) that was supplemented with 5% fetal bovine serum
600 (FBS) Superior (Biochrom, Germany), 2% chicken serum (ThermoFisher Scientific, USA)
601 and 1% Penicillin-Streptomycin-Solution (Penicillin 10,000 U/ml and Streptomycin 10

602 mg/ml) (Biochrom. Germany). Subsequently, CEFs were incubated at 40°C in a 5% CO2
603 atmosphere until infection. The infection of CEFs with an H9N2 virus (A/chicken/Saudi
604 Arabia/CP7/1998) was done after overnight seeding 250.000 cells/well in 6 well plates and
605 infecting them in three independent experiments with multiplicities of infection (MOIs) of
606 0.1 and 1. Supernatants were collected 24h post-infection from the infected cells and
607 titrated on MDCK (kindly provided by Prof. Silke Rautenschlein, University of Veterinary
608 Medicine, Hannover). The virus titration was done as previously described (48). An
609 additional *in vitro* infection experiment with CEFs was conducted using the H1N1-WSN
610 strain (A/WSN/1933), kindly provided by Prof. Bernd Kaspers, Ludwig Maximilian
611 University of Munich. Briefly, cells of the four genotypes were seeded overnight and
612 infected with two different MOIs, 0.001 and 0.01. 40h later, they were fixed and stained
613 for plaque formation following the standard titration protocol(48).

614 ***In ovo* infection of embryonated eggs**

615 Fertilized eggs from a crossing of *RIG-I* (+/-) and *RNF135*(+/-) were collected and
616 incubated till ED10 or ED14. In a blind study, eggs were infected randomly with 10^3 FFU
617 of the H9N2 virus, as previously described (56). 24h post-infection, the allantois fluid and
618 muscle tissue were collected respectively for viral titration and genotyping. The virus
619 titration was done on MDCK cells as previously described (48).

620 **RT-PCR for the detection of transgene expression in different tissues**

621 RNA from chicken organs, including lung, trachea, heart, liver, duodenum, thymus, bursa,
622 and brain, was isolated with Reliaprep RNA Tissue Miniprep System according to
623 manufacturer instructions (Promega), followed by cDNA synthesis using GoScript
624 Reverse transcription mix (Promega). The detection of *RIG-I*, as well as *RNF135* from
625 various tissues, was done using the following primers. *RIG-I*: 613_RIG-I-for (5'-
626 CCTAGGAGAAGCATTCAAGGAG-3') and 563_RIG-I_Rev 5'-
627 (CTAAAATGGTGGGTACAAGTTGGAC-3'), while *RNF135* was detected using the
628 following primers: 898_duRNF_for (5'-CTTGAGAGAGGTGGAGGGAGC-3') and
629 899_duRNF_rev (5'-GGGCTGGTGGGAATTGTTGAGG-3'). *RIG-I* and *RNF135* PCRs
630 produced an amplicon of 298bp and 148bp, respectively. β-actin mRNA was detected with
631 primers Beta_actin_F (5′-TACCACAATGTACCCTGGC-3′) and Beta_actin_R (5′-
632 CTCGTCTTGTTTTATGCGC-3′) (57), resulting in a 300-bp amplicon. The PCR was

633 performed using FIREPol DNA Polymerase (Solis Bio-dyne) according to the
634 manufacturer's instructions. The following PCR conditions were used: initial denaturation
635 at 98 °C 30 sec, followed by 40 cycles of 98 °C 10 sec, 59 °C 30 sec, 72 °C 30 sec, and
636 a final extension step of 72 °C 2 min.

637 **Metanalysis of *RIG-I* and *RNF135* expression in duck tissues**

638 A metanalysis of publicly available RNA-seq data was performed to estimate the
639 expression of *RIG-I* and *RNF135* in duck tissues (reads per kilobase per million mapped
640 reads; RPKM), as previously described (58).

641 **Enzyme-linked immunosorbent assay (ELISA)**

642 ELISA was done to measure the total plasma IgM and IgY concentrations. Briefly, 96 well
643 plates were coated overnight with anti-chicken antibodies IgM and IgY at a concentration
644 of 2µg/mL (Supplementary Table 1). The next day, plates were washed three times with
645 washing buffer, followed by a blocking step with 4% skim milk for one hour. The prediluted
646 plasma samples in 1:3 serial dilution were pipetted in the plates and incubated for one
647 hour. The detection was done using secondary HRP-conjugated antibodies at the
648 concentrations mentioned in Tabe1, which were incubated for 1h at RT. This was followed
649 by adding 100µl/well of TMB (3,3', 5,5;-tetramethylbenzidine) substrate solution for 10 min,
650 which was stopped by 50µl per well of 1M sulfuric acid solution. The optical density (OD)
651 was measured using FluoStar Omega via the measuring filter 450nm and the reference
652 filter 620 nm (Version 5.70 R2 BMG LABTECH, Ortenberg, Germany).

653 **Flow Cytometry**

654 Peripheral blood mononuclear cells (PBMCs) were isolated using Histopaque®-1077
655 density gradient centrifugation (Sigma, Taufkirchen, Germany) and analyzed using flow
656 cytometry. Extracellular staining was carried out to detect various chicken immune cell
657 markers including T cell subpopulations, B cells and Monocytes (list of antibodies is
658 mentioned in Supplementary Table 1). Briefly, $5x10^6$ cells were washed with 2% BSA
659 diluted in PBS (FLUO-Buffer). To determine the living cell population, cells were incubated
660 with Fixable Viability Dye eFluor 780 (eBioscience, Thermo Fisher Scientific, USA). After
661 washing with FLUO-Buffer, primary antibodies (concentration shown in Supplementary
662 Table 1) were applied for 20 min. Cells were washed in FLUO-Buffer to remove unbound

663 antibodies and incubated with conjugated secondary antibodies for 20 min. Subsequently,
664 cells were again washed and analyzed using an Attune flow cytometer (Thermo Fisher
665 Scientific, USA). The obtained data were then analyzed with FlowJo 10.8.1 software
666 (FlowJo, Ashland, USA). An example of the gating strategy used in this study is presented
667 in Supplementary Figure 12.

668 **Assessment of *in vitro* T cell activation**

669 PBMCs were isolated from 12-weeks-old *RIG-I* or WT birds and resuspended in RPMI
670 medium supplemented with 10%FBS and 1% Penicillin/Streptomycin and distributed on a
671 48 well plate with a total of $5x10^6$ cells/well. Cells were subsequently stimulated with
672 Concanavalin A (Con A) (eBioscience™) at a concentration of 25 µg per well. They were
673 monitored every 24h for T cell activation via flow cytometry. Activated T cells were stained
674 for surface expression of γδTCR1, CD25, or αβTCR2&3 using antibodies listed in
675 Supplementary Table 1.

676 **Challenge infection experiment with H7N1**

677 The challenge infection experiment was performed at the INRAE-PFIE platform (INRAE
678 Centre Val de Loire, Nouzilly, France) and approved by the local Ethics Committee Val de
679 Loire and the Ministère de l' Enseignement Supérieur et de la Recherche under the
680 number 2021120115599580. Transgenic birds required for the experiment were hatched
681 in dedicated hatching isolators and genotyped by PCR using DNA extracted from EDTA
682 blood samples collected at day 7 post hatch. At 3 weeks of age, transgenic and WT-
683 chickens were distributed into four different groups (Supplementary Table 3)
684 corresponding to four BSL-3 isolator units. Two other groups were kept together as MOCK
685 controls in a single isolator (Supplementary Table 3). The birds were fed a commercial
686 standard diet and provided water ad libitum throughout the experiment. Prior to infection
687 (0 dpi), body weights were recorded, and blood samples were taken by occipital sinus
688 puncture. The virus used for challenge infection was A/ Turkey/Italy/977/1999 (kindly
689 provided by Dr. Ilaria Capua, Istituto Zooprofilattico Sperimentale Delle Venezie, Legnaro,
690 Italy), an H7N1 subtype virus that, despite its classification as an LPAIV, causes up to
691 50% mortality in experimentally infected White Leghorn chickens (24, 59, 60).

692 Chickens were PBS/mock-treated (groups 5 and 6) or virus-infected (groups 1-4) by intra-
693 tracheal and intra-choanal cleft inoculation of 0.1mL PBS or $5x10^5$ EID50/$1x10^6$ EID50
694 H7N1. Animal behavior and clinical disease signs were monitored twice daily during the
695 trial. Clinical signs were evaluated according to the following score: 0 (no clinical signs), 1
696 (mild clinical signs), 2 (severe clinical signs), or 3 (dead/euthanized). Birds were
697 euthanized by pentobarbital injection into the occipital sinus at the end of the experiment
698 or once humane endpoints were reached. Samples collected from euthanized birds
699 included lung, caeca, and spleen. In addition, a scoring system was used to evaluate
700 macroscopic lung lesions as follows: 1 (mild, localized edema and fibrinous exudate), 2
701 (moderate edema and with hemorrhage and fibrinous exudate over ~1/4 of the lung), or 3
702 (severe hemorrhage and extensive edema over ~1/2 of the lung) (Supplementary Figure
703 13). Data collected from the animal experiment were assessed at 2 and 6 dpi, representing
704 the time points when tissue samples for the Fluidigm assay were collected. Details
705 regarding the number of birds, group distribution and number of analyzed samples are
706 given in Supplementary Tables 3 and 4.

707 **Quantification of the viral genome in H7N1-challenged chickens**

708 Total RNA was isolated from the isolated organs and conserved in 1ml NucleoProtect
709 RNA (Macherey-Nagel, Germany). Samples were later processed for total RNA isolation
710 with NucleoSpin RNA (Macherey-Nagel, Germany) according to the manufacturer's
711 instructions. The viral genome of the H7N1 virus was quantified using qRT-PCR that was
712 conducted with the Bio-Rad iTaq™ Universal SYBR ® Green One-Step Kit (BioRad,
713 California, USA) using primers designed for the detection of the M gene as published
714 elsewhere (61).

715 **Analysis of gene expression via Fluidigm Dynamic Array**

716 Gene expression was analyzed as previously described (25). Briefly, total RNA was
717 extracted from infected animals' lungs, caeca, and spleen and processed for quality
718 control via nanodrop. Reverse transcription was performed using the High Capacity
719 Reverse Transcription Kit (Applied Biosystems) according to manufacturer's instructions
720 with random hexamers and oligo (dT)18 in a final volume of 10µl, containing 250 ng total
721 RNA. Subsequently, the cDNA was pre-amplified using TaqMan PreAmp Master Mix
722 (Applied Biosystems). Quantitative PCR was performed in the BioMark HD instrument with

723 the 96.96 IFC Dynamic Array (Fluidigm). The reaction was prepared by mixing 2.5 µl
724 TaqMan Gene Expression Master Mix (Applied Biosystems), 0.25 µl 20X DNA Binding
725 Dye Sample Loading Reagent (Fluidigm), 0.25 µl 20X EvaGreen DNA binding dye
726 (Biotum) and 2 µl of preamplified cDNA. The qPCR was run under the following thermal
727 conditions: 50°C for 2 min, 70°C for 30 min, 25°C for 10 min, followed by hot start 50°C
728 for 2 min, 95°C for 10 min, PCR (x30 cycles) 95°C for 15 sec, 60°C for 60 sec and melting
729 curve analysis 60°C for 3 sec to 95°C.

730 Raw quantitation cycle (Cq) data were collated with the Real-time PCR Analysis software
731 v3.1.3 (Fluidigm), setting parameters of quality Cq threshold to auto (global) and the
732 baseline correction to derivative. Raw Cq values were processed with GenEx.v6 MultiD,
733 with correction for primer efficiency and reference gene normalization. Stability of the
734 expression of reference genes: *TATA box binding protein (TBP), Tubulin alpha chain*
735 *(TUBA8B), beta-actin (ACTB), beta-glucuronidase (GUSB), glyceraldehyde-3-phosphate*
736 *dehydrogenase (GAPDH) and ribosomal 28S (r28S)* were evaluated via NormFinder
737 (GenEx). The geometric mean of the most stable (*GAPDH*, *GUSB* and *TBP*) were used
738 for normalization. Technical replicates were averaged, and relative quantification was to
739 the maximum Cq value obtained per gene, transformed to logarithmic scale, which was
740 then statistically analyzed using T-test.

741 **Challenge infection experiments with H3N1 and H9N2**

742 Challenge experiments were performed at the Animal Research Center (ARC) of the
743 Technical University of Munich and approved by the government of Upper Bavaria under
744 the number ROB- 55.2-2532.Vet_02-21-11. The H3N1 virus
745 (A/Chicken/Belgium/460/2019) was kindly provided by Dr. Joris Pieter De Gussem
746 (Poulpharm BV). Infection with H3N1 was done with 28-week-old chickens. Infection with
747 H9N2 (A/chicken/Saudi Arabia/CP7/1998) was done with four weeks old chicks. According
748 to the obtained genotype at hatch (WT, *RIG-I-* and *RIG-I-RNF135*-expressing chickens),
749 birds were distributed to groups of four or six birds per group. An infectious dose of 10^6
750 FFU in 0.2mL PBS per bird was distributed via nasal and tracheal routes for both viruses.
751 In both experiments, birds were monitored daily for clinical symptoms, and tracheal swabs
752 were collected on days 0, 3, 7, 11 and 17 to analyze the viral RNA loads by RT-qPCR(48).
753 Duodenum, lung, and spleen samples were collected when mortality occurred or on the

754 final day of the experiment (17 dpi). The expression of *RIG-I*, *RNF135*, *IFN-γ, IFN-α, IL1β,*
755 *and IL6* was assessed by RT-qPCR (62).

756 **Histology**

757 Caeca and lungs (H7N1 infection experiment) or oviduct samples (infundibulum, magnum
758 – H3N1 infection experiment) were fixed in 10% neutral buffered formalin and processed
759 routinely. Four-micrometer tissue sections were stained with hematoxylin and eosin for
760 light microscopy. The sections' analysis addressed histopathological changes and signs
761 of inflammatory reactions, including degeneration, necrosis, infiltration of inflammatory
762 cells, fibrin exudation, and epithelial hyperplasia.

763 **Statistical analysis**

764 Statistical analysis was done using IBM SPSS Statistics (Version 28.0.1.1. IBM, Armonk,
765 USA). The normality of the data was examined via Kolmogorov-Smirnov and Shapiro-Wilk
766 tests. The comparison between two groups was made either with Two Samples T-test or
767 Wilcoxon Signed Rank test. Multiple group comparison was made using Kruskal-Wallis
768 Test or with One-Way ANOVA. The statistical test result was considered significant when
769 the *P* value was less than 0.05.

770
771 **Acknowledgments**
772
773 Animal husbandry and experimental infrastructure was provided by the TUM Animal Research
774 Center (ARC). The authors thank the animal keepers of the ARC as well as the team at the INRAE
775 Plateforme d'Infectiologie Expérimentale (INRAE-PFIE, Nouzilly, France) for conducting the H7N1
776 challenge infection experiment. Additionally, the authors thank the technical staff of the involved
777 laboratories for excellent assistance.

778 **Funding**

779 The project was financed by a grant from the German Research Foundation to H.S. (DFG SI
780 2478/2-1). B. Schusser was funded by the DFG in the framework of the Research Unit
781 ImmunoChick (FOR5130) project SCHU2446/6-1. MNA was funded by the Alexander von
782 Humboldt Foundation (Ref 3.5 - 1222975 - IND - HFST-P) and the German Research Foundation
783 under the Walter Benjamin Programme (Project number AL2729/1-1). In addition, the H7N1
784 challenge infection experiment was supported by the European infrastructure project VetBioNet

785 (EU Horizon 2020, grant agreement No 731014). L.V. was supported by the Biotechnology and
786 Biological Sciences Research Council Institute Strategic Program Grant funding
787 (BBS/E/D/30002276).

788 **References**
789

790 1. A. Mostafa, E. M. Abdelwhab, T. C. Mettenleiter, S. Pleschka, Zoonotic potential of
791 influenza A viruses: a comprehensive overview. *Viruses* **10**, 497 (2018).
792 2. E. F. S. Authority *et al.*, Avian influenza overview December 2022-March 2023. *EFSA*
793 *journal. European Food Safety Authority* **21**, e07917 (2023).
794 3. G. Granata, L. Simonsen, N. Petrosillo, E. Petersen, Mortality of H5N1 human infections
795 might be due to H5N1 virus pneumonia and could decrease by switching receptor. *The*
796 *Lancet Infectious Diseases* **24**, e544-e545 (2024).
797 4. M. Kang *et al.*, Changing epidemiological patterns in human avian influenza virus
798 infections. *The Lancet Microbe* **5** (2024).
799 5. N. MacLachlan, Orthomyxoviridae. *Fenner's veterinary virology*, 353-370 (2011).
800 6. J. K. Kim, N. J. Negovetich, H. L. Forrest, R. G. Webster, Ducks: the "Trojan horses" of
801 H5N1 influenza. *Influenza and other respiratory viruses* **3**, 121-128 (2009).
802 7. M. R. Barber, J. R. Aldridge Jr, R. G. Webster, K. E. Magor, Association of RIG-I with
803 innate immunity of ducks to influenza. *Proceedings of the National Academy of Sciences*
804 **107**, 5913-5918 (2010).
805 8. J. Rehwinkel *et al.*, RIG-I detects viral genomic RNA during negative-strand RNA virus
806 infection. *Cell* **140**, 397-408 (2010).
807 9. E. Kowalinski *et al.*, Structural basis for the activation of innate immune pattern-
808 recognition receptor RIG-I by viral RNA. *Cell* **147**, 423-435 (2011).
809 10. M. Yoneyama *et al.*, The RNA helicase RIG-I has an essential function in double-stranded
810 RNA-induced innate antiviral responses. *Nature immunology* **5**, 730-737 (2004).
811 11. M. U. Gack *et al.*, TRIM25 RING-finger E3 ubiquitin ligase is essential for RIG-I-mediated
812 antiviral activity. *Nature* **446**, 916-920 (2007).
813 12. D. Gao *et al.*, REUL is a novel E3 ubiquitin ligase and stimulator of retinoic-acid-inducible
814 gene-I. *PloS one* **4**, e5760 (2009).
815 13. H. Oshiumi *et al.*, The ubiquitin ligase Riplet is essential for RIG-I-dependent innate
816 immune responses to RNA virus infection. *Cell host & microbe* **8**, 496-509 (2010).
817 14. Y. Wang *et al.*, Rig-I−/− mice develop colitis associated with downregulation of Gαi2. *Cell*
818 *research* **17**, 858-868 (2007).
819 15. I. K. Pang, P. S. Pillai, A. Iwasaki, Efficient influenza A virus replication in the respiratory
820 tract requires signals from TLR7 and RIG-I. *Proceedings of the National Academy of*
821 *Sciences* **110**, 13910-13915 (2013).
822 16. R. Cagliani *et al.*, RIG-I-like receptors evolved adaptively in mammals, with parallel
823 evolution at LGP2 and RIG-I. *Journal of molecular biology* **426**, 1351-1365 (2014).
824 17. M. Kandasamy *et al.*, RIG-I signaling is critical for efficient polyfunctional T cell responses
825 during influenza virus infection. *PLoS pathogens* **12**, e1005754 (2016).
826 18. H. A. Vanderven *et al.*, Avian influenza rapidly induces antiviral genes in duck lung and
827 intestine. *Molecular immunology* **51**, 316-324 (2012).

828 19. W. Zheng, Y. Satta, Functional evolution of avian RIG-I-like receptors. *Genes* **9**, 456
829 (2018).
830 20. V. Krchlíková *et al.*, Dynamic Evolution of Avian RNA Virus Sensors: Repeated Loss of
831 RIG-I and RIPLET. *Viruses* **15**, 3 (2022).
832 21. T. J. Hayman *et al.*, RIPLET, and not TRIM25, is required for endogenous RIG-I-dependent
833 antiviral responses. *Immunology and cell biology* **97**, 840-852 (2019).
834 22. Y. Xiao, M. B. Reeves, A. F. Caulfield, D. Evseev, K. E. Magor, The core promoter controls
835 basal and inducible expression of duck retinoic acid inducible gene-I (RIG-I). *Molecular*
836 *immunology* **103**, 156-165 (2018).
837 23. C. Cadena *et al.*, Ubiquitin-dependent and-independent roles of E3 ligase RIPLET in
838 innate immunity. *Cell* **177**, 1187-1200. e1116 (2019).
839 24. W. G. Dundon, A. Milani, G. Cattoli, I. Capua, Progressive truncation of the Non-
840 Structural 1 gene of H7N1 avian influenza viruses following extensive circulation in
841 poultry. *Virus research* **119**, 171-176 (2006).
842 25. K. J. Bryson *et al.*, Comparative Analysis of Different Inbred Chicken Lines Highlights How
843 a Hereditary Inflammatory State Affects Susceptibility to Avian Influenza Virus. *Viruses*
844 **15**, 591 (2023).
845 26. J. de Wit *et al.*, Major difference in clinical outcome and replication of a H3N1 avian
846 influenza strain in young pullets and adult layers. *Avian pathology* **49**, 286-295 (2020).
847 27. J. Guan, Q. Fu, S. Sharif, Replication of an H9N2 avian influenza virus and cytokine gene
848 expression in chickens exposed by aerosol or intranasal routes. *Avian Diseases* **59**, 263-
849 268 (2015).
850 28. H. Kato *et al.*, Differential roles of MDA5 and RIG-I helicases in the recognition of RNA
851 viruses. *Nature* **441**, 101-105 (2006).
852 29. L. Xu, D. Yu, Y. Fan, Y.-P. Liu, Y.-G. Yao, Evolutionary selection on MDA5 and LGP2 in the
853 chicken preserves antiviral competence in the absence of RIG-I. *Journal of Genetics and*
854 *Genomics= Yi Chuan xue bao* **46**, 499-503 (2019).
855 30. D. Evseev, D. Miranzo-Navarro, X. Fleming-Canepa, R. G. Webster, K. E. Magor, Avian
856 Influenza NS1 Proteins Inhibit Human, but Not Duck, RIG-I Ubiquitination and Interferon
857 Signaling. *Journal of Virology* **96**, e00776-00722 (2022).
858 31. A. Iwamoto, H. Tsukamoto, H. Nakayama, H. Oshiumi, E3 Ubiquitin Ligase Riplet Is
859 Expressed in T Cells and Suppresses T Cell–Mediated Antitumor Immune Responses. *The*
860 *Journal of Immunology* **208**, 2067-2076 (2022).
861 32. M. Elsheimer-Matulova *et al.*, Interleukin 4 inducible 1 gene (IL4I1) is induced in chicken
862 phagocytes by Salmonella Enteritidis infection. *Veterinary Research* **51**, 1-8 (2020).
863 33. S. A. Nish *et al.*, T cell-intrinsic role of IL-6 signaling in primary and memory responses.
864 *elife* **3**, e01949 (2014).
865 34. D. T. Thoresen, D. Galls, B. Götte, W. Wang, A. M. Pyle, A rapid RIG-I signaling relay
866 mediates efficient antiviral response. *Molecular cell* **83**, 90-104. e104 (2023).
867 35. J. Cornelissen, J. Post, B. Peeters, L. Vervelde, J. Rebel, Differential innate responses of
868 chickens and ducks to low-pathogenic avian influenza. *Avian Pathology* **41**, 519-529
869 (2012).
870 36. N. P. Liau *et al.*, The molecular basis of JAK/STAT inhibition by SOCS1. *Nature*
871 *communications* **9**, 1558 (2018).
872 37. D. C. Palmer, N. P. Restifo, Suppressors of cytokine signaling (SOCS) in T cell
873 differentiation, maturation, and function. *Trends in immunology* **30**, 592-602 (2009).

874 38. C. Vazquez, C. Y. Tan, S. M. Horner, Hepatitis C virus infection is inhibited by a
875 noncanonical antiviral signaling pathway targeted by NS3-NS4A. *Journal of Virology* **93**,
876 e00725-00719 (2019).
877 39. T. Schmit *et al.*, Interferon-γ promotes monocyte-mediated lung injury during influenza
878 infection. *Cell reports* **38** (2022).
879 40. M. G. Koliopoulos *et al.*, Molecular mechanism of influenza A NS1-mediated TRIM25
880 recognition and inhibition. *Nature communications* **9**, 1820 (2018).
881 41. N. R. Meyerson *et al.*, Nuclear TRIM25 specifically targets influenza virus
882 ribonucleoproteins to block the onset of RNA chain elongation. *Cell host & microbe* **22**,
883 627-638. e627 (2017).
884 42. M. Okamoto, T. Kouwaki, Y. Fukushima, H. Oshiumi, Regulation of RIG-I activation by
885 K63-linked polyubiquitination. *Frontiers in immunology* **8**, 1942 (2018).
886 43. H. Fischer, E. Tschachler, L. Eckhart, Pangolins lack IFIH1/MDA5, a cytoplasmic RNA
887 sensor that initiates innate immune defense upon coronavirus infection. *Frontiers in*
888 *immunology* **11**, 939 (2020).
889 44. H. Oshiumi, M. Matsumoto, T. Seya, Ubiquitin-mediated modulation of the cytoplasmic
890 viral RNA sensor RIG-I. *The journal of biochemistry* **151**, 5-11 (2012).
891 45. Y. Chen *et al.*, Duck RIG-I CARD domain induces the chicken IFN-β by activating NF-κB.
892 *Biomed Research International* **2015** (2015).
893 46. B. Rieblinger *et al.*, Strong xenoprotective function by single-copy transgenes placed
894 sequentially at a permissive locus. *Xenotransplantation* **25**, e12382 (2018).
895 47. J. S. Long *et al.*, Species specific differences in use of ANP32 proteins by influenza A
896 virus. *Elife* **8**, e45066 (2019).
897 48. H. Sid, S. Hartmann, C. Winter, S. Rautenschlein, Interaction of influenza A viruses with
898 oviduct explants of different avian species. *Frontiers in Microbiology* **8**, 1338 (2017).
899 49. M.-C. Van de Lavoir *et al.*, Interspecific germline transmission of cultured primordial
900 germ cells. *PLoS One* **7**, e35664 (2012).
901 50. M.-C. Van de Lavoir *et al.*, Germline transmission of genetically modified primordial
902 germ cells. *Nature* **441**, 766-769 (2006).
903 51. P. A. Leighton, M. C. van de Lavoir, J. H. Diamond, C. Xia, R. J. Etches, Genetic
904 modification of primordial germ cells by gene trapping, gene targeting, and φC31
905 integrase. *Molecular Reproduction and Development: Incorporating Gamete Research*
906 **75**, 1163-1175 (2008).
907 52. V. Hamburger, H. L. Hamilton, A series of normal stages in the development of the chick
908 embryo. *Journal of morphology* **88**, 49-92 (1951).
909 53. J. Whyte *et al.*, FGF, insulin, and SMAD signaling cooperate for avian primordial germ
910 cell self-renewal. *Stem cell reports* **5**, 1171-1182 (2015).
911 54. B. Schusser *et al.*, Immunoglobulin knockout chickens via efficient homologous
912 recombination in primordial germ cells. *Proceedings of the National Academy of*
913 *Sciences* **110**, 20170-20175 (2013).
914 55. R. Hernandez, D. T. Brown, Growth and maintenance of chick embryo fibroblasts (CEF).
915 *Current protocols in microbiology* **17**, A. 4I. 1-A. 4I. 8 (2010).
916 56. R. Brauer, P. Chen, Influenza virus propagation in embryonated chicken eggs. *JoVE*
917 *(Journal of Visualized Experiments)*, e52421 (2015).

57. F.-k. Kong, C.-l. H. Chen, A. Six, R. D. Hockett, M. D. Cooper, T cell receptor gene deletion circles identify recent thymic emigrants in the peripheral T cell pool. *Proceedings of the National Academy of Sciences* **96**, 1536-1540 (1999).
58. N. B. Burkhardt *et al.*, The long pentraxin PTX3 is of major importance among acute phase proteins in chickens. *Frontiers in Immunology* **10**, 124 (2019).
59. I. Monne *et al.*, Emergence of a highly pathogenic avian influenza virus from a low-pathogenic progenitor. *Journal of virology* **88**, 4375-4388 (2014).
60. S. Trapp *et al.*, Major contribution of the RNA-binding domain of NS1 in the pathogenicity and replication potential of an avian H7N1 influenza virus in chickens. *Virology journal* **15**, 1-12 (2018).
61. C. Ward *et al.*, Design and performance testing of quantitative real time PCR assays for influenza A and B viral load measurement. *Journal of clinical virology* **29**, 179-188 (2004).
62. T. von Heyl *et al.*, Loss of αβ but not γδ T cells in chickens causes a severe phenotype. *European Journal of Immunology* **53**, 2350503 (2023).

952 **Figures**

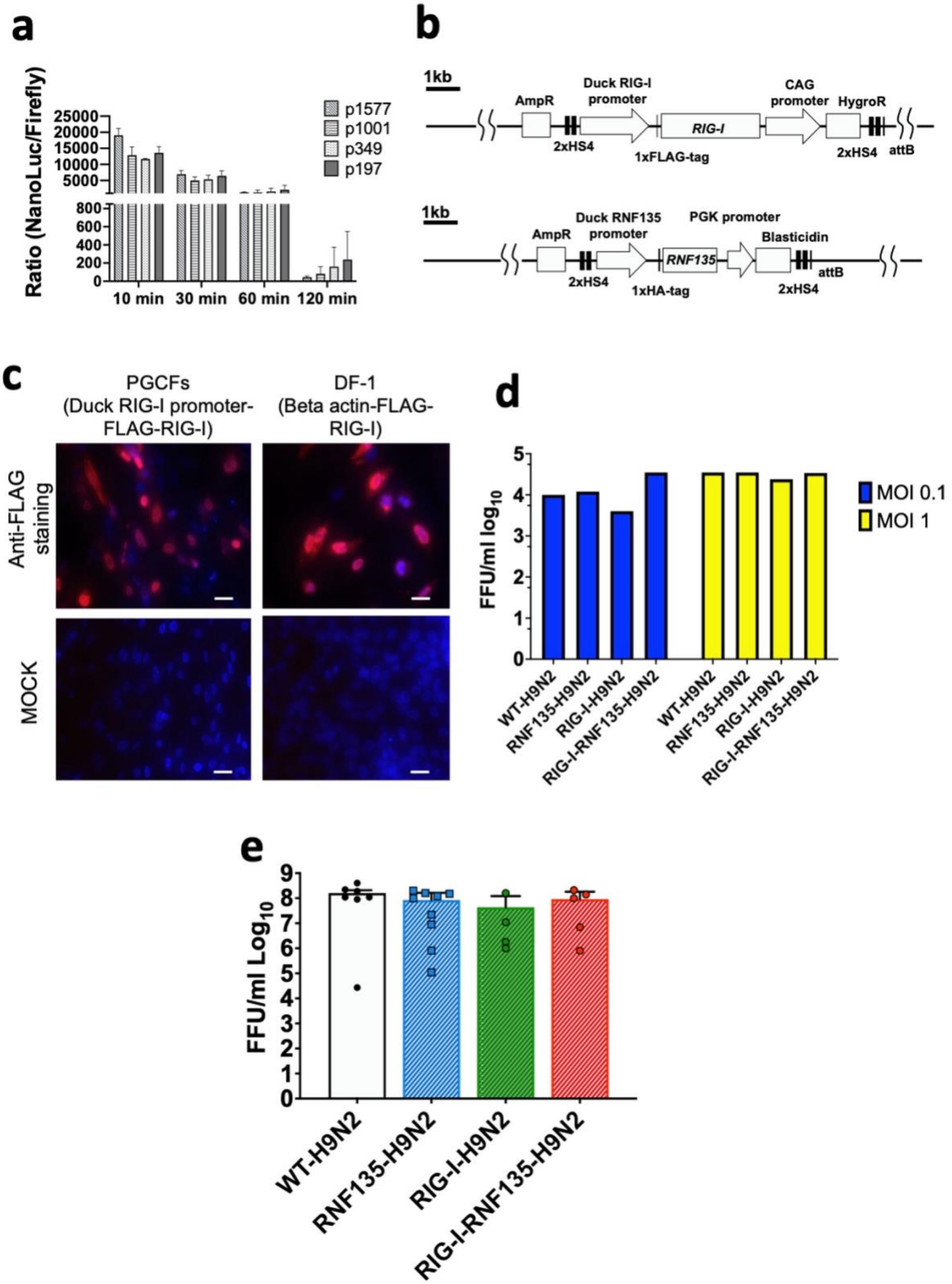

953

954 **Figure 1. Generation of PGCs and susceptibility to infection using *in vitro* and *in***
955 ***vivo* systems. a.** Promoter activity of the duck *RNF135* was examined by generating
956 different deletion mutants tested in chicken DF-1 cells; the promoter activity was then
957 evaluated by measuring the NanoLuc/Firefly ratio (n=3). **b.** Diagram of both constructs
958 used to generate *RIG-I*-expressing chicken (upper diagram), using the previously
959 identified duck *RIG-I* promoter (22) , and *RNF135*-expressing chickens (lower diagram),
960 using the duck *RNF135* promoter, whose activity was identified in this study. **c.** Primordial
961 germ cells (PGCs) that express the duck *RIG-I* under the duck *RIG-I* promoter were
962 derived into PGC fibroblasts (PGCFs) and were infected later with avian influenza virus
963 H9N2 to stimulate *RIG-I* expression upon influenza infection; the cells were infected for
964 18h with low pathogenic avian influenza virus H9N2 and subsequently stained for FLAG-
965 Tag (red staining); MOCK control represents uninfected cells, and were not positive for
966 anti-FLAG-Tag; DF-1 cells that express the FLAG-tagged duck *RIG-I* under the chicken
967 beta-actin promoter were used as a positive control (red staining). **d.** Quantification of
968 newly produced viral particles after infection of CEFs; CEFs were isolated from different
969 transgenic embryos and experimentally infected with LPAIV H9N2 at two different
970 multiplicities of infection (MOI 0.1 and 1); Supernatants were collected at 24hpi and titrated
971 on MDCK cells; no significant differences were observed between the groups (p>0.05). **e.**
972 Quantification of newly produced viral particles after infection of embryonated eggs. 10-
973 day-old embryonated eggs were infected with LPAIV H9N2 at 10^3 FFU/egg; allantois fluid
974 was collected 24hpi and titrated on MDCK cells; no significant differences were observed
975 between the groups (p>0.05). Error bars indicate the standard error of mean (SEM);
976 Depending on the normal distribution of the data, multiple group comparison was done
977 either with one-way ANOVA or Independent-Samples Kruskal-Wallis Test

978

979

980

981

982

983

984

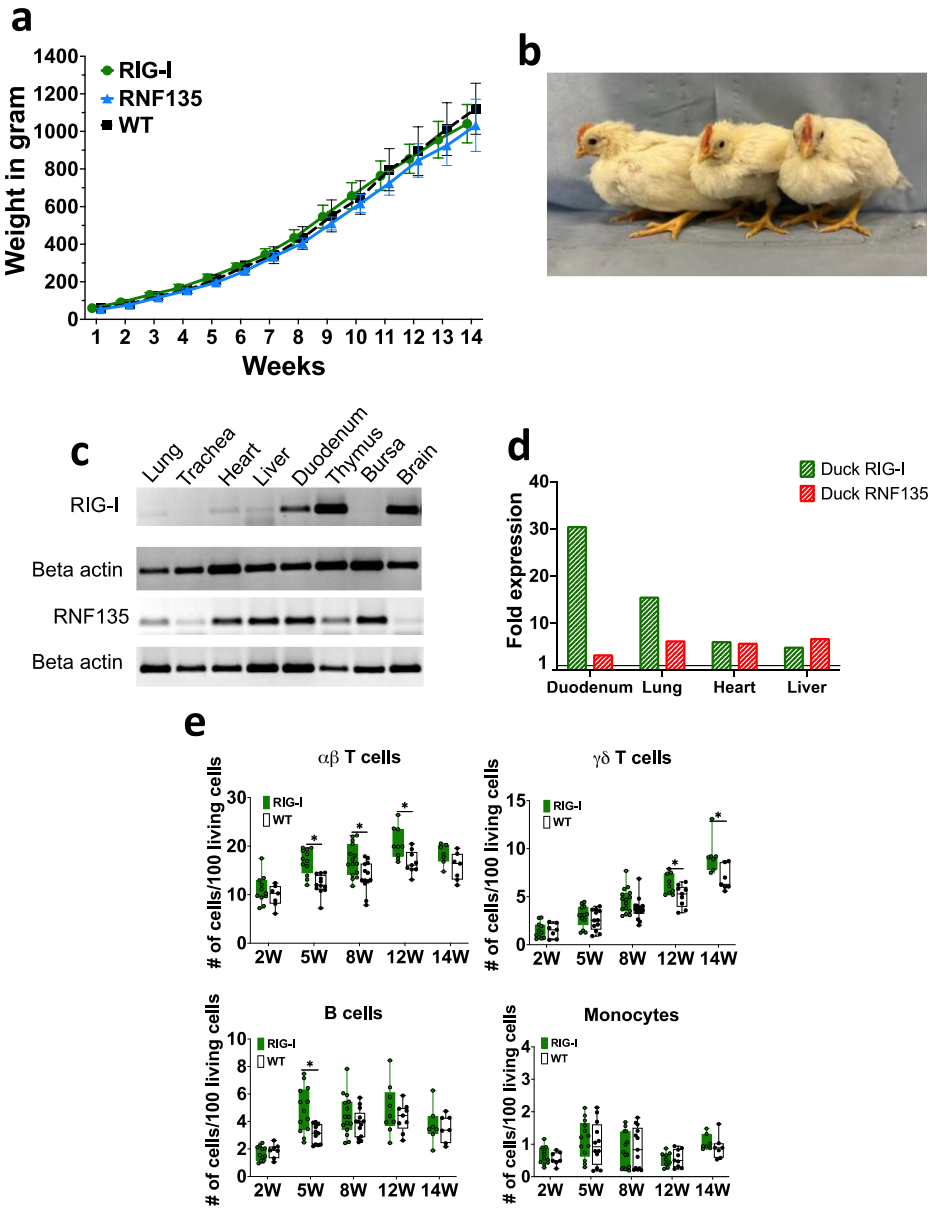

985

986 **Figure 2. Generation and immunophenotypic characterization of *RIG-I* and *RNF135*-**
987 **expressing chickens. a.** Weekly weight monitoring of the generated heterozygous birds
988 (p>0.05) (n=10). **b.** Representative picture of the generated heterozygous birds from left
989 to right at four weeks of age: WT, *RNF135*-expressing chicken, and *RIG-I*-expressing
990 chicken. **c.** RT-PCR of the transgenic expression of *RIG-I* and *RNF135* in different organs.
991 **d.** Analysis of duck RIG-I and duck RNF135 expression in various tissues using reads per
992 kilobase per million mapped reads (RPKM). **e.** Assessment of different immune cell

populations in *RIG-I*-expressing chickens compared to their WT siblings. (*) indicates statistical differences between groups tested simultaneously ($p<0.05$). Depending on the normal distribution of the data, two-group comparison was done with the Wilcoxon rank-sum test or two two-sample T-test

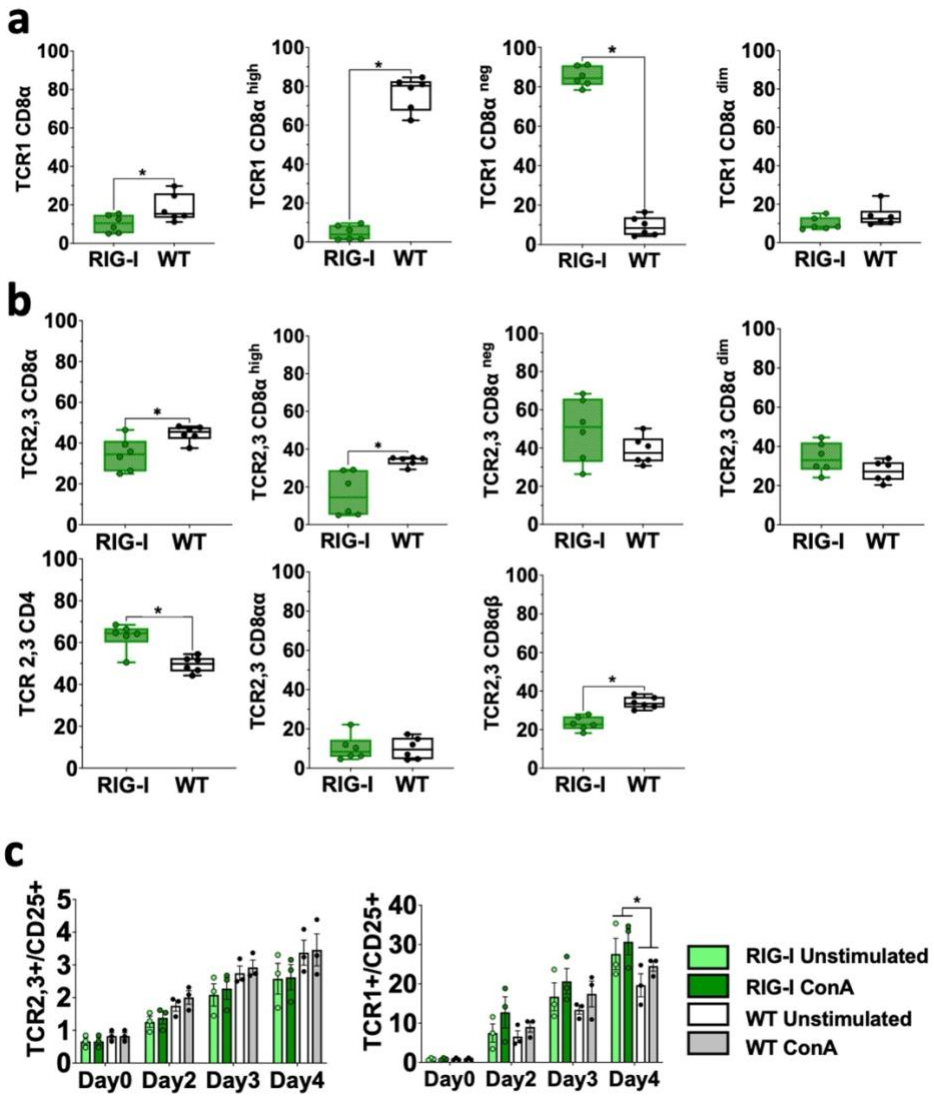

Figure 3. Assessment of different T cell subpopulations in *RIG-I*-expressing chickens compared to their WT siblings

a. PBMCS were analyzed for γδTCR1+/CD8α+ T cells at 12 weeks. B) PBMCS were analyzed for αβTCR2,3+T cells and CD4+ or CD8α+T cells at 12 weeks ($p<0.05$). **c.** Activation of isolated T cells from 12-week-old *RIG-I*-expressing chickens compared to

1004 their WT siblings ($p<0.05$); cells were sorted according to their TCR expression, stimulated
1005 with Concanavalin A, and quantified by flow cytometry at different time-points. The Y-axis
1006 depicts the number of positive cells per 100 viable TCR+ cells. Error bars indicate the
1007 standard error of mean (SEM); (*) indicate statistical differences between groups tested
1008 simultaneously ($p<0.05$). Depending on the normal distribution of the data, two-group
1009 comparison was done with the Wilcoxon rank-sum test or two-sample T-test, while multiple
1010 group comparison was done either with one-way ANOVA or Independent-Samples
1011 Kruskal-Wallis Test

1012

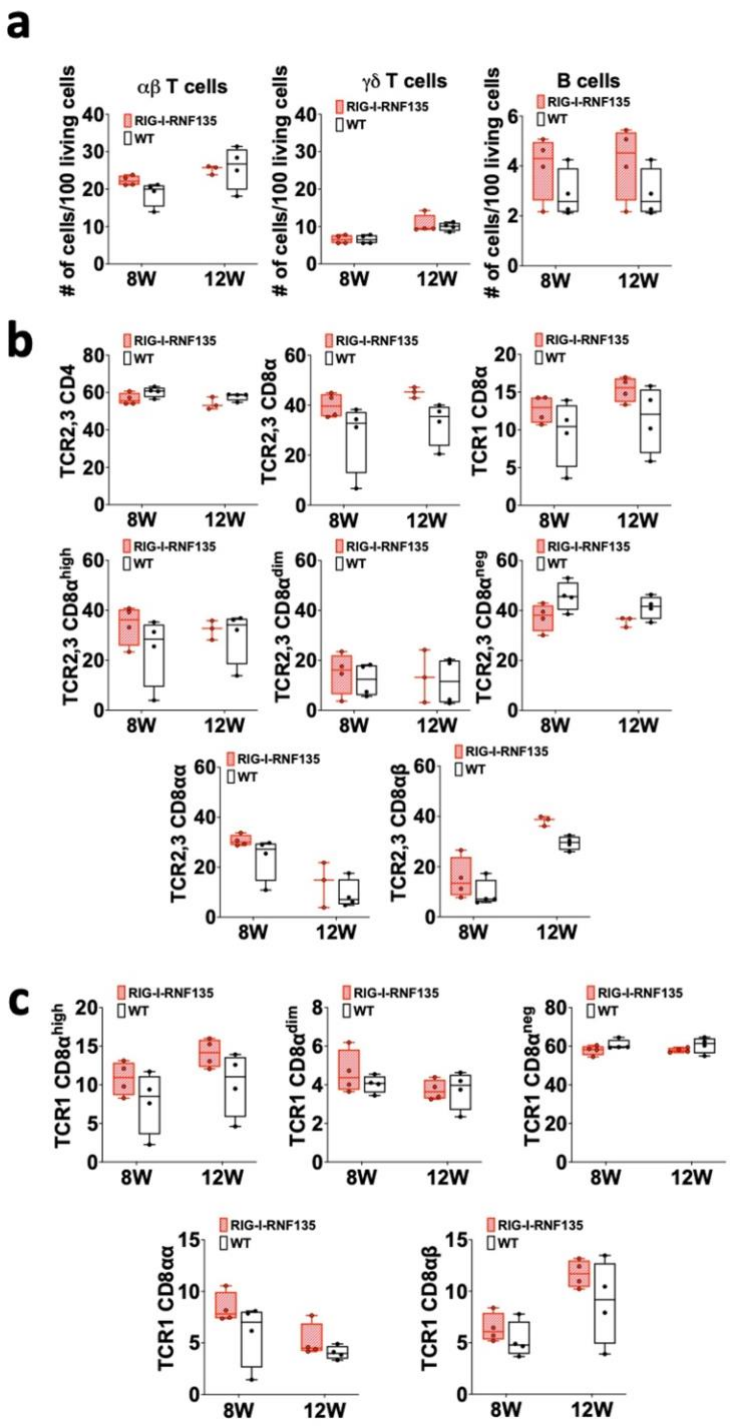

1013

1014 **Figure 4. Simultaneous expression of *RIG-I* and *RNF135* in the chicken does not**
1015 **lead to differences in the adaptive immune phenotype compared to WT birds**

1016 Two-time points, eight and twelve weeks of age, were chosen based on the data obtained
1017 from *RIG-I*-expressing chickens to assess the immunophenotype of *RIG-I-RNF135*-
1018 expressing chickens. PBMCS were isolated and analyzed for B cells, αβTCR2,3+ or
1019 γδTCR1 + T cells (**a**) as well as for CD4+ (B) and CDα8+ T cells (**c**). No significant
1020 differences were detected between the analyzed groups (p>0.05). Depending on the
1021 normal distribution of the data, two-group comparison was done with the Wilcoxon rank-
1022 sum test or two-sample T-test

1023

1024

1025

1026

1027

1028

1029

1030

1031

1032

1033

1034

1035

1036

1037

1038

1039

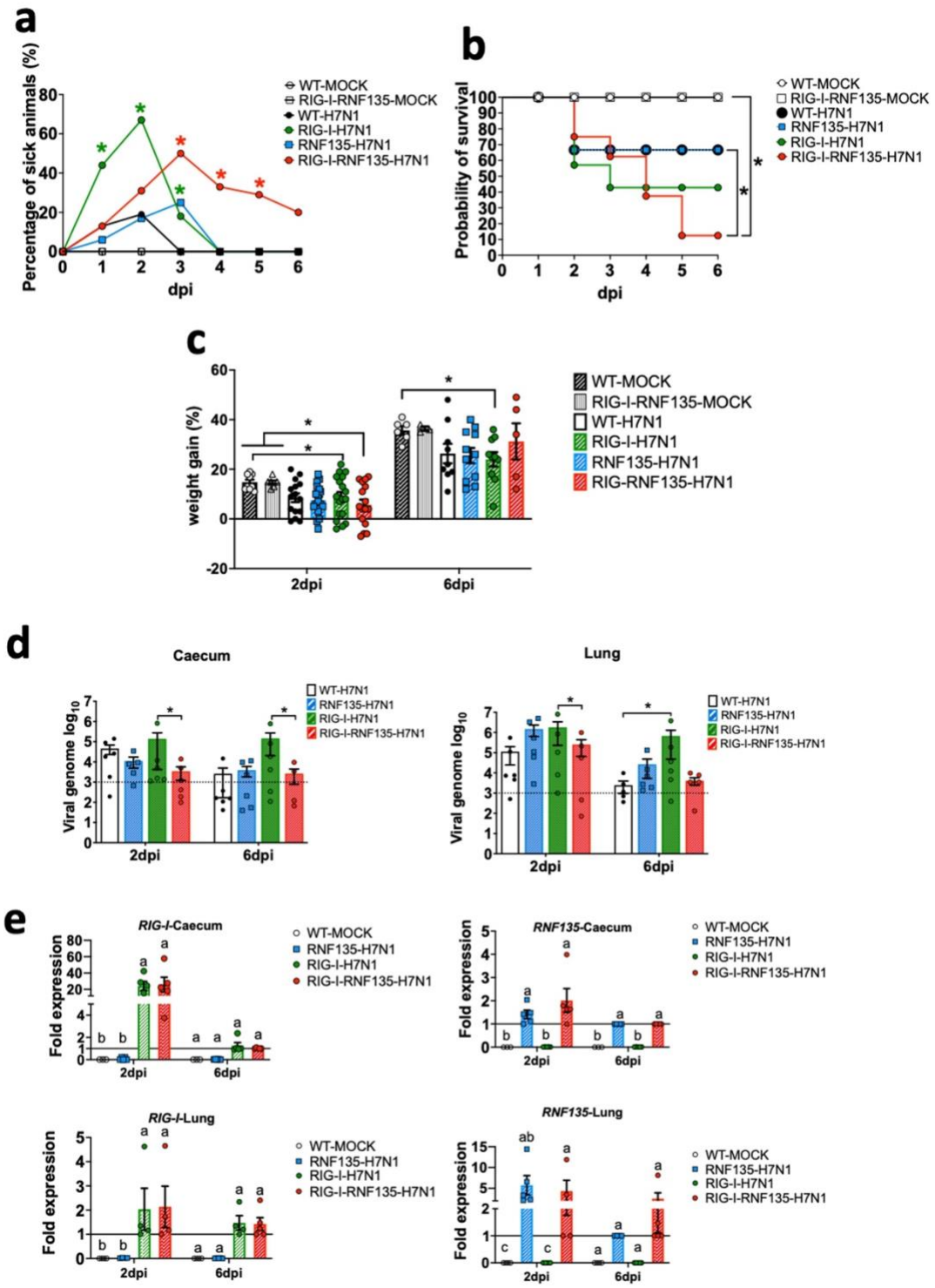

1040

1041 **Figure 5. H7N1-challenge experiment reveals the susceptibility of *RIG-I*-expressing**
1042 **chickens and the role of *RNF135* in effective *RIG-I* antiviral response.**

1043 The generated transgenic chickens were challenged with H7N1 and assessed at two days
1044 post-infection (dpi) and six dpi for different parameters. **a.** Percentage of animals
1045 presenting clinical symptoms. **b.** Probability of survival in the challenged groups. **c.** Weight
1046 gain in challenged groups compared to WT- and *RIG-I-RNF135*-MOCK- controls ($p<0.05$).
1047 **d.** Viral replication rate in two main target organs, caecum, and lung ($p<0.05$); the
1048 horizontal line indicates the detection threshold of the PCR based on the signal obtained
1049 from the uninfected controls, which is $\log_{10}(10^3)$. **e.** Expression levels of transgenes in the
1050 caecum and the lung upon H7N1-challenge. Error bars indicate standard error of mean
1051 (SEM); (*) or different letters indicate statistical differences between groups tested
1052 simultaneously ($p<0.05$). Depending on the normal distribution of the data, multiple group
1053 comparison was done either with one-way ANOVA or Independent-Samples Kruskal-
1054 Wallis Test

1055

1056

1057

1058

1059

1060

1061

1062

1063

1064

1065

1066

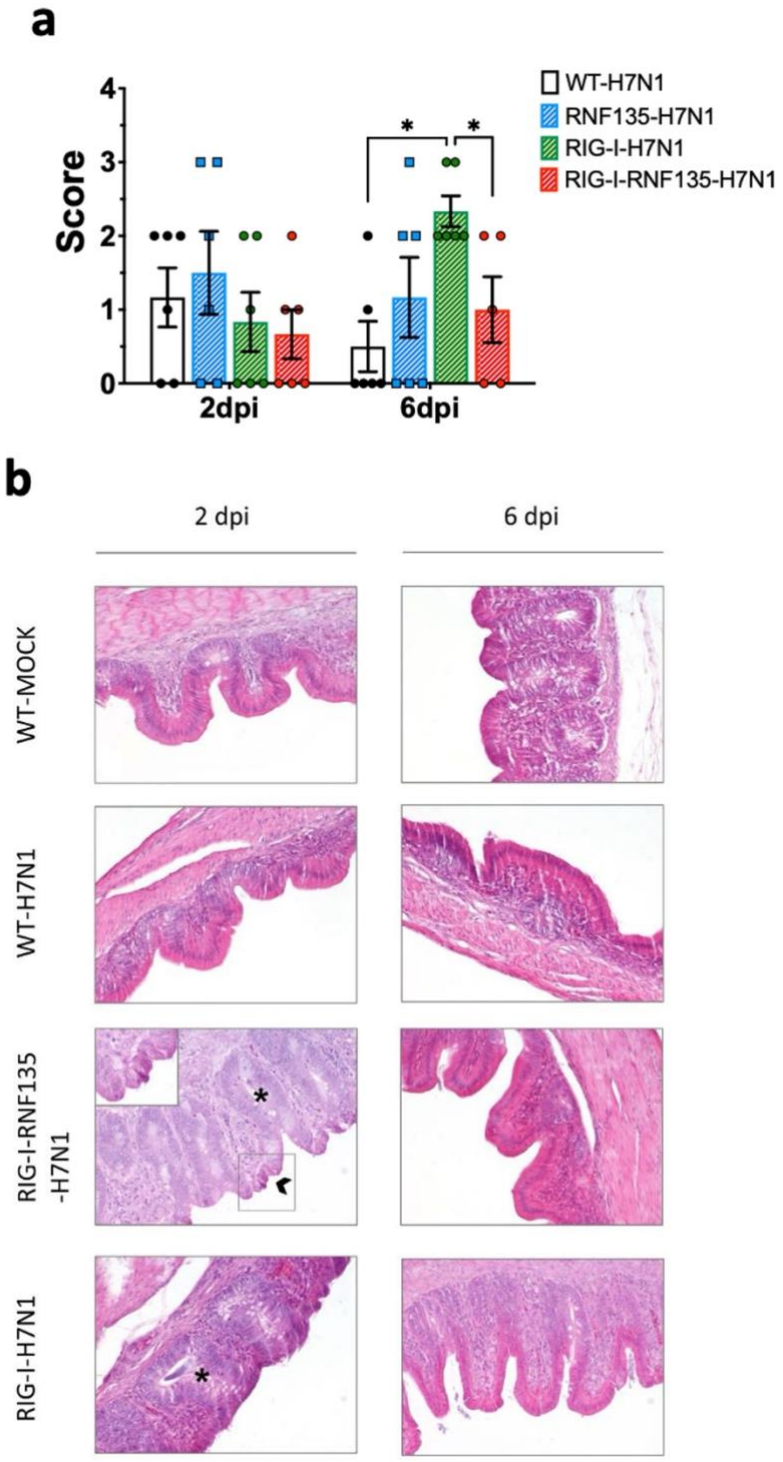
a
Score
4
3
2
1
0
2dpi
6dpi
*
*
WT-H7N1
RNF135-H7N1
RIG-I-H7N1
RIG-I-RNF135-H7N1
b
2 dpi
6 dpi
WT-MOCK
WT-H7N1
RIG-I-RNF135
-H7N1
RIG-I-H7N1
*
*

1067

1068

1069 **Figure 6. Developed lesions in H7N1-challenged birds a.** Macroscopical lesion score
1070 of the lungs showing a significant increase of lesions in *RIG-I*-expressing birds at six dpi
1071 ($p<0.05$) **b.** Histology of the caecum showing the typical structure of the epithelium in the
1072 control groups. *RIG-I-RNF135* challenged birds showed epithelial hyperplasia with
1073 necrosis that diminished by 6 dpi. *RIG-I*-expressing chickens did not show necrotic lesions
1074 but pronounced epithelial hyperplasia that lessened by six dpi. Asterix indicates epithelial
1075 hyperplasia with the mitotic figures, while the arrow indicates necrotic epithelial cells; 200x.
1076 Error bars indicate standard error of mean (SEM); (*) indicate statistical differences
1077 between groups tested simultaneously ($p<0.05$). Depending on the normal distribution of
1078 the data, multiple group comparison was done either with one-way ANOVA or
1079 Independent-Samples Kruskal-Wallis Test

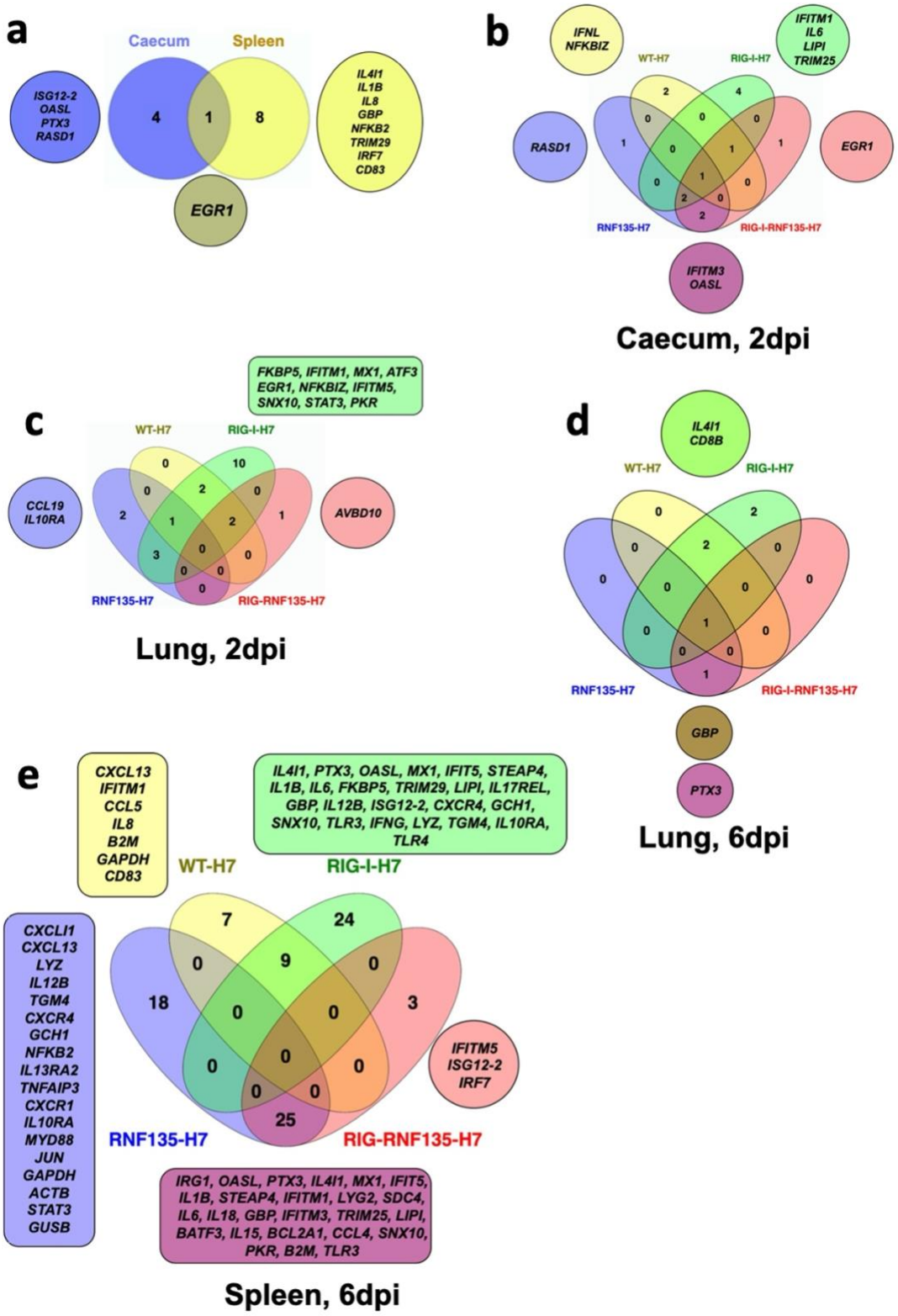
a
Caecum
Spleen
ISG12-2
OASL
PTX3
RASD1
4
1
8
IL4I1
IL1B
IL8
GBP
NFKB2
TRIM29
IRF7
CD83
EGR1
b
IFNL
NFKBIZ
IFITM1
IL6
LIPI
TRIM25
WT-H7
RIG-I-H7
RASD1
EGR1
RNF135-H7
RIG-I-RNF135-H7
IFITM3
OASL
Caecum, 2dpi
c
FKBP5, IFITM1, MX1, ATF3
EGR1, NFKBIZ, IFITM5,
SNX10, STAT3, PKR
WT-H7
RIG-I-H7
CCL19
IL10RA
AVBD10
RNF135-H7
RIG-RNF135-H7
Lung, 2dpi
d
IL4I1
CD8B
WT-H7
RIG-I-H7
RNF135-H7
RIG-I-RNF135-H7
GBP
PTX3
Lung, 6dpi
e
CXCL13
IFITM1
CCL5
IL8
B2M
GAPDH
CD83
WT-H7
IL4I1, PTX3, OASL, MX1, IFIT5, STEAP4,
IL1B, IL6, FKBP5, TRIM29, LIPI, IL17REL,
GBP, IL12B, ISG12-2, CXCR4, GCH1,
SNX10, TLR3, IFNG, LYZ, TGM4, IL10RA,
TLR4
RIG-I-H7
CXCLI1
CXCL13
LYZ
IL12B
TGM4
CXCR4
GCH1
NFKB2
IL13RA2
TNFAIP3
CXCR1
IL10RA
MYD88
JUN
GAPDH
ACTB
STAT3
GUSB
IFITM5
ISG12-2
IRF7
RNF135-H7
RIG-RNF135-H7
IRG1, OASL, PTX3, IL4I1, MX1, IFIT5,
IL1B, STEAP4, IFITM1, LYG2, SDC4,
IL6, IL18, GBP, IFITM3, TRIM25, LIPI,
BATF3, IL15, BCL2A1, CCL4, SNX10,
PKR, B2M, TLR3
Spleen, 6dpi

1080

1081 **Figure 7. Infection of transgenic chickens with H7N1 leads to upregulated**
1082 **inflammatory genes.** Venn diagram of fluidigm qRT-
1083 PCR array of naive and challenged birds with H7N1 showing significantly upregulated
1084 genes in various organs. Significant DEGs were identified by comparing the relative
1085 expression values for every chicken line to the WT-MOCK individually per timepoint, with
1086 a significance level set at $p < 0.05$; fold change >1 (n ≥ 5-time point). **a.** Upregulated genes
1087 in *RIG-I-RNF135*-expressing chickens without infection **b.** Upregulated genes in the
1088 caecum between H7N1-challenged groups at 2dpi **c.** Upregulated genes in the lung
1089 between H7N1-challenged groups at 2dpi **d.** Upregulated genes in the lung between
1090 H7N1-challenged groups at 6dpi **e.** Upregulated genes in the spleen between H7N1-
1091 challenged groups at 6dpi

1092

1093

1094

1095

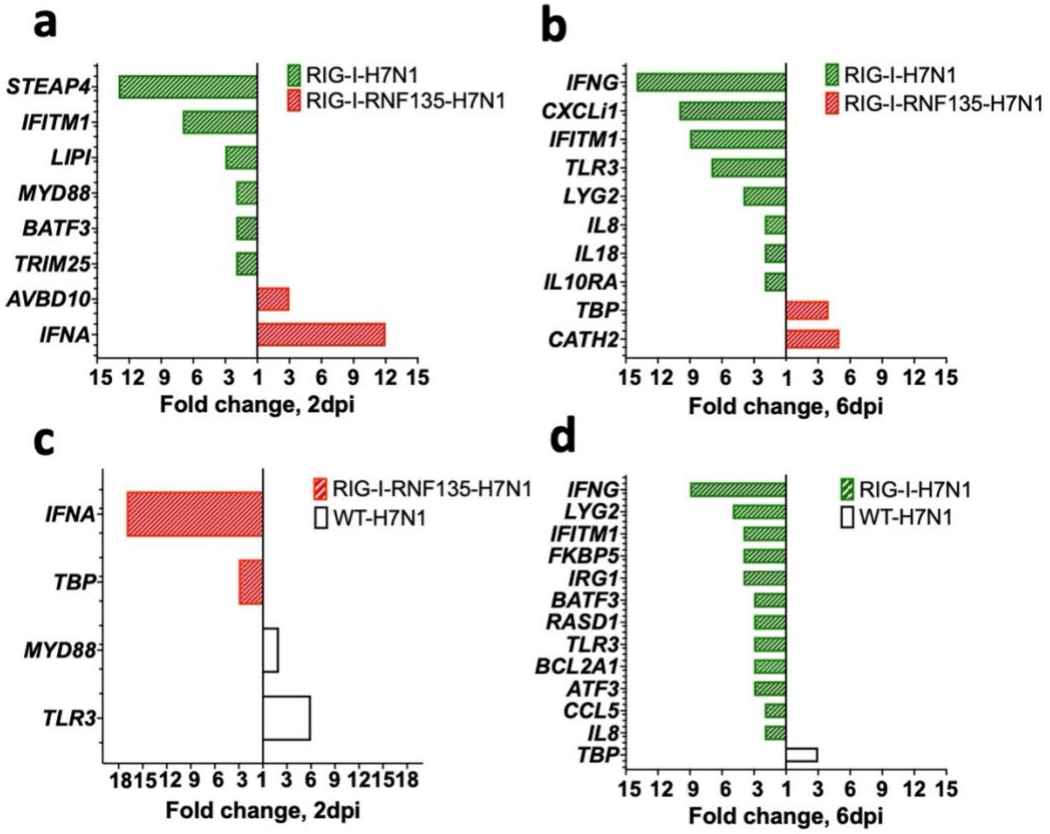

Figure 8. Gene expression in the lung upon H7N1-infection

Significant DEGs were identified by using Fluidigm qPCR array and comparison of the relative expression values between H7N1-challenged groups. **a.** Significantly upregulated genes after comparison of infected *RIG-I-* with *RIG-I-RNF135*-expressing chickens at two dpi. **b.** Significantly upregulated genes after comparison of infected *RIG-I*-with *RIG-I-RNF135*-expressing chickens at 6dpi. **c.** Significantly upregulated genes after comparison of infected *RIG-I-* with *RIG-I-RNF135*-expressing chickens at two dpi. **d.** Significantly upregulated genes after comparison of infected *RIG-I*-expressing with infected WT-chickens at six dpi. Significance levels were set at $p < 0.05$; fold change >1 (n ≥ 5-time point)

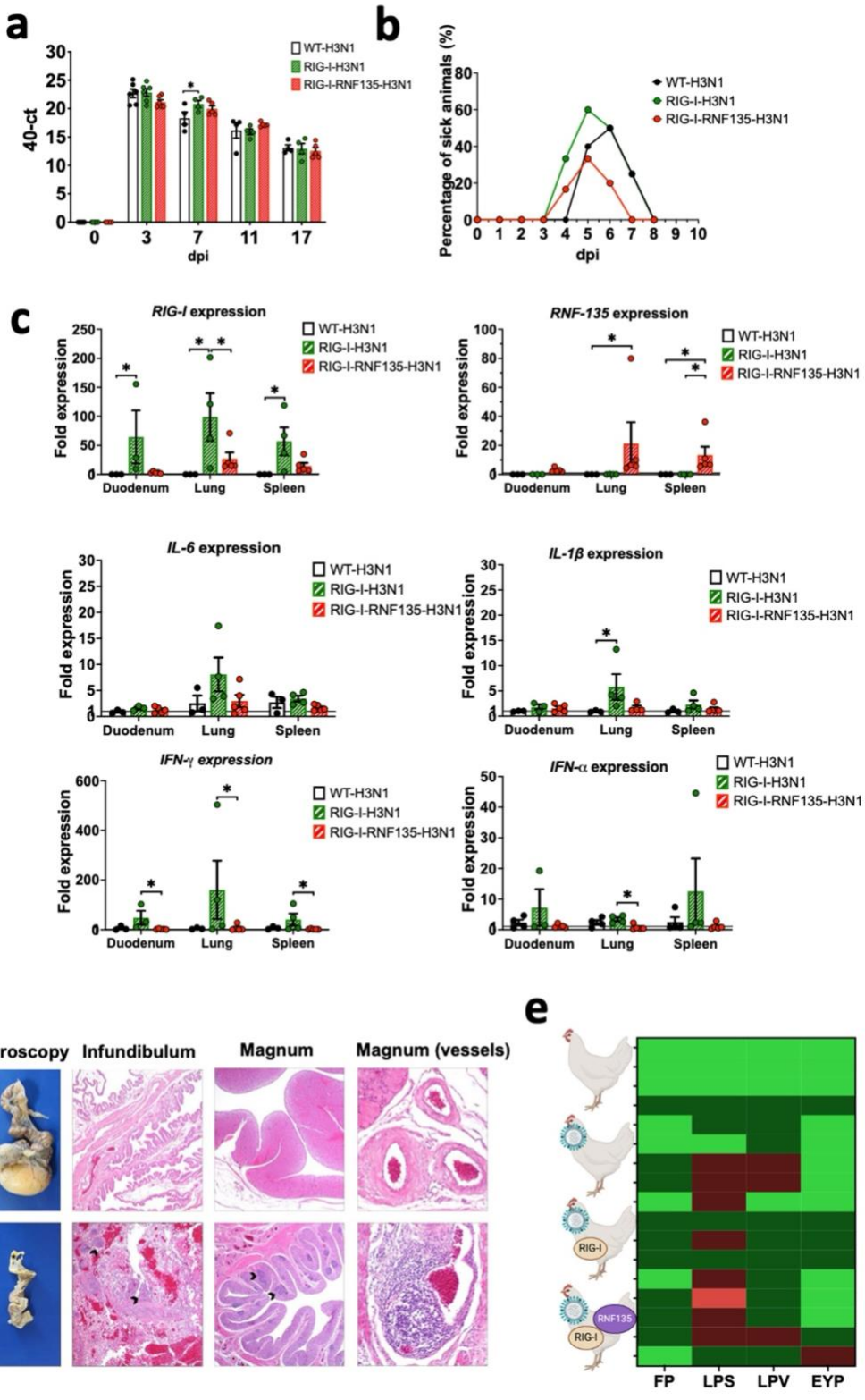
a
WT-H3N1
RIG-I-H3N1
RIG-I-RNF135-H3N1
40-ct
dpi
b
Percentage of sick animals (%)
dpi
c
RIG-I expression
RNF-135 expression
IL-6 expression
IL-1β expression
IFN-γ expression
IFN-α expression
Fold expression
Duodenum
Lung
Spleen
d
Macroscopy
Infundibulum
Magnum
Magnum (vessels)
WT-MOCK
RIG-I-RNF135-H3N1
e
RIG-I
RNF135
FP
LPS
LPV
EYP

1110

1111 **Figure 9. H3N1-challenge experiment confirms the exacerbated disease phenotype**
1112 **of *RIG-I* and *RIG-I-RNF135* chickens infected with virulent avian influenza viruses**

1113 The generated transgenic chickens were challenged at 28 weeks of age with H3N1 and
1114 assessed for different parameters. **a.** Viral shedding based on tracheal swabbing and viral
1115 RNA load analysis. b. Probability of survival in the challenged groups. **c.** Expression of
1116 *RIG-I*, *RNF135*, and influenza-regulated genes in the duodenum, lung, and spleen. **d.**
1117 Histological assessment of the reproductive tract; WT-MOCK: normal macroscopical and
1118 histological appearance of the salpinx; RNF-RIG-I-H3N1: severe atrophy with mild
1119 fibrinous peritonitis in the infundibulum (asterisk), severe lymphoplasmacytic salpingitis
1120 (arrowheads) (40x), the magnum (20x), and vasculitis in the magnum vessels (200x). **e.**
1121 Scoring of lesions in the reproductive tract in all challenged groups, starting with the upper
1122 row WT-MOCK, WT-H3N1, *RIG-I*-H3N1, and *RIG-I-RNF135*-H3N1; FP: fibrinous
1123 peritonitis, LPS: lymphoplasmacytic salpingitis, LPV: lymphoplasmacytic vasculitis, EYP:
1124 egg yolk peritonitis. Error bars indicate standard error of mean (SEM); (*) indicate
1125 statistical differences between groups tested simultaneously ($p<0.05$). Depending on the
1126 normal distribution of the data, multiple group comparison was done either with one-way
1127 ANOVA or Independent-Samples Kruskal-Wallis Test